Technical Assistance Consultant's Report

Project No: 42384-012
September 2020

Knowledge and Innovation Support for ADB's Water Financing Program

Remote Sensing Based Water Productivity Assessment – Vennar and Cauvery Subbasin, Tamil Nadu

Prepared by

International Water Management Institute

For Asian Development Bank

ASIAN DEVELOPMENT BANK

Remote Sensing Based Water Productivity Assessment – Vennar and Cauvery Subbasin, Tamil Nadu

FINAL REPORT

IWMI International Water Management Institute

CGIAR RESEARCH PROGRAM ON Water, Land and Ecosystems

ADB

Project final report submitted to the Asian Development Bank under the program for Expanding support to Water Accounting in River Basins and Water Productivity in Irrigation Schemes.

Citation: Velpuri, N.M., Khan, A., and Rebelo, L-M., 2020. Remote Sensing Based Water Productivity Assessment –. Project report, Vennar and Cauvery Subbasin, Tamil Nadu, IWMI, Colombo, Sri Lanka

Cover image: Sprinkler irrigation, India, Hamish John Appleby / IWMI

EXPANDING SUPPORT TO WATER ACCOUNTING IN RIVER BASINS AND WATER PRODUCTIVITY IN IRRIGATION SCHEMES

Project final report:

Remote Sensing Based Water Productivity Assessment, Vennar and Cauvery Subbasin, Tamil Nadu

PREPARED FOR THE
ASIAN DEVELOPMENT BANK
BY

The International Water Management Institute

September 2020

TABLE OF CONTENTS

List of Figures

List of Tables

List of abbreviations

ADB	Asian Development Bank
AGBP	Above Ground Biomass Production
CAVSCDP	Climate Adaptation in Vennar subbasin in Cauvery Delta Project
CDZ	Cauvery Delta Zone
CWP	Crop Water Productivity
CWSI	Crop Water Stress Index
DSS	Decision Support System
ETa	Actual Evapotranspiration
FAO	Food and Agriculture Organization
GEE	Google Earth Engine
GLDAS	Global Land Data Assimilation System
HI	Harvest Index
IHE Delft	IHE Delft Institute for Water Education
IWMI	International Water Management Institute
MODIS	Moderate Resolution Imaging Spectroradiometer
NASA	National Aeronautics and Space Administration
NDVI	Normalized difference vegetation index
PySEBAL	Python implementation of SEBAL
RWD	Relative Water Deficit
SRTM	Shuttle Radar Topography Mission
TA	Technical Assistance
WP	Water Productivity

I. INTRODUCTION

1. The ADB is committed under its Water Operational Plan 2011-2020 to undertake expanded and enhanced analytical work to enable its developing member countries to secure deeper and sharper understanding of water issues and solutions. IHE Delft, in collaboration with IWMI and FAO, will support ADB in achieving this objective.

2. The activities proposed under the current study build on the work previously undertaken by IHE Delft and IWMI in cooperation with the Asian Development Bank (ADB) to assess crop water productivity and to assess water resource status in selected countries in Asia.

3. Through the current study, IHE Delft in collaboration with its subcontracted partner, IWMI, will support (a) ADB's lending and non-lending assistance in the water sector, and (b) the design of irrigation projects at an early stage at selected candidate projects.

4. IHE Delft and IWMI aim to support ADB's lending and non-lending assistance in the water sector by creating (i) comprehensive, (ii) comprehensible, and (iii) accessible information on available water resources and their current uses in major river basins. IHE Delft and IWMI aim to support the design of, or investments in irrigation schemes at project start by (i) providing baseline data for parameters related to land and water productivity, and (ii) identifying suitable interventions.

5. Assistance is being provided to Projects in 7 countries, with two sites in India. The nature of the support provided in each is determined through close consultation with ADB Project Officers, and tailored to the individual project requirements. In some locations, this may take the form of water accounting assessments to characterize water use and availability, while in others emphasis may be placed on water productivity (either crop or biomass water productivity), or on irrigation performance assessments, to target investments.

6. This document is the Final Report the activities undertaken by IWMI to support the 'Climate Adaptation in Vennar subbasin in Cauvery Delta Project' (CAVSCDP) in Tamil Nadu. The activities are in the following referred to as "the study".

II. PROJECT BACKGROUND

7. In 2012 the Government of India outlined the National Water Policy 2012; this recognizes numerous water resource issues in the country and proposes the introduction of modern water resources management principles and best practices to address them.

8. The Water Resources Department (WRD)[1], Government of Tamil Nadu, is tasked with the overall management of Tamil Nadu's water resources, and has initiated several projects to address state-wide water resources availability and management challenges.

[1] Part of the Public Works Department

9. The Climate Adaptation through Subbasin Development Program (CASDP) project, implemented through the WRD, is one of these. CASDP has been designed to address rehabilitation of the irrigation infrastructure and improved water resources management in the Cauvery River subbasin, and to make structural and non-structural climate adaptations in the water sector in the Cauvery Basin in Tamil Nadu. By doing so, it supports the implementation of the Government of India's National Action Plan on Climate Change (NAPCC) of 2008 and the National Water Mission (NWM).

10. As a part of CASDP, the Government of Tamil Nadu has received financing from the Asian Development Bank (ADB) for implementing the Climate Adaptation in Vennar Subbasin in Cauvery Delta Project (CAVSCDP). ADB approved the Project (CAVSCDP; Loan-3394-IND) on 7 June 2016 for $100 million to be implemented over 5 years.

11. CAVSCDP aims to modernize irrigation and flood management infrastructure in six of the main river channels, and to establish improved management systems to help local communities in the Vennar River command area in the Cauvery Delta Zone (CDZ) of Tamil Nadu. This is being achieved by upgrading irrigation infrastructure, focusing on structural adaptations for optimal use of surface water to ensure that as many areas of the Cauvery delta as possible are served with irrigation water equally and efficiently.

12. Activities also include the preparation of a follow on project, referred to as "Project 2". Project 2 will cover the remaining rivers channels and streams in the Vennar and Cauvery subbasins that were not covered in Project 1. This follow-on project will include priority areas across the entire river network and its structures under the main channels in both the Vennar and the Cauvery subbasin.

13. During the CAVSCD Project inception it was reported that many of the irrigation structures are old and poorly maintained, affecting the reliability of surface water supplies (PTAC 2018). As a result, farmers in the lower delta resort to groundwater pumping, and over extraction of this has contributed to saltwater intrusion and salinization of freshwater supplies; high salinity of groundwater also affects crop yields. The objective of the project is thus to make agriculture more sustainable through both structural and nonstructural interventions.

III. SCOPE OF SERVICES

14. During the Inception Phase of the study, it was agreed that IWMI would work with ADB to provide support to the CAVSCDP.

15. On the 22-28th June 2019, IWMI joined the CAVSCDP Loan Review Mission[2] in Tamil Nadu, in order to gain a detailed understanding of the project and to define the scope of services to be provided.

[2] The Inception Workshop for the current TA

16. Initial discussions during the mission focused on the Vennar command areas (also referred to in the CAVSCDP as the "Vennar subbasin"), which covers an area of 4,154 km^2 (see Map C, Figure 1).

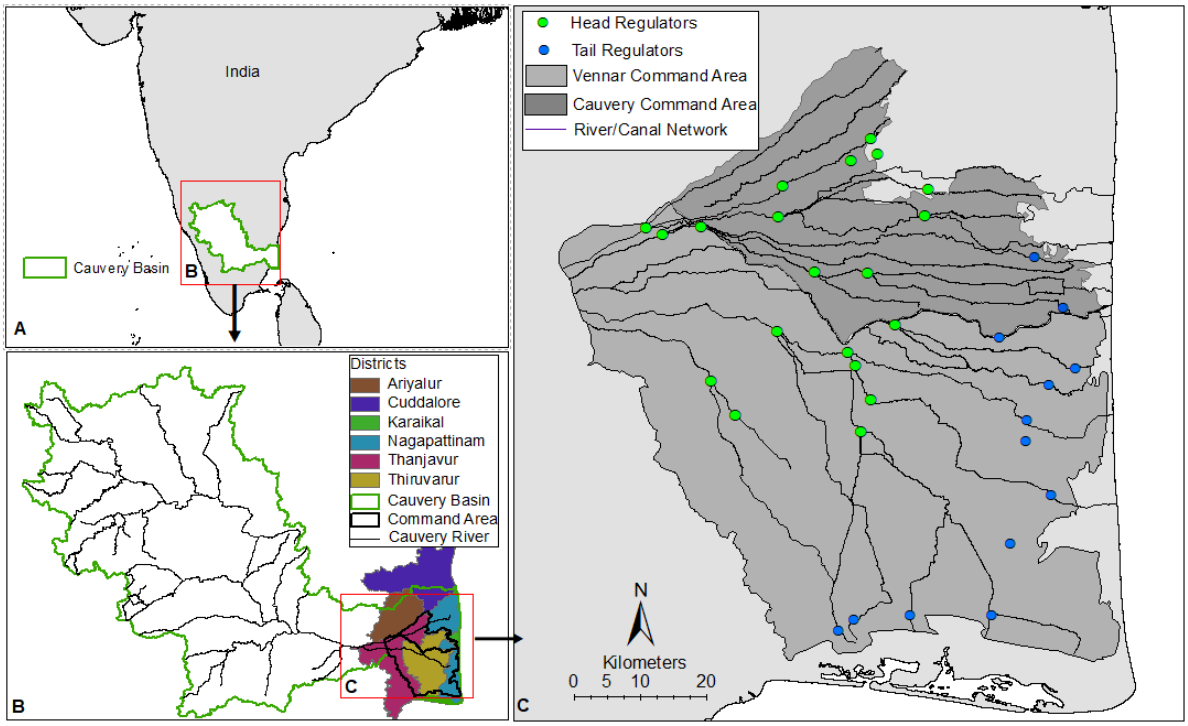

Figure 1: Location of the Cauvery River and Cauvery and Vennar command areas within the Cauvery Delta Zone (CDZ; Source: IWMI estimates).

17. Following the mission and subsequent discussions with ADB, IWMI agreed to undertake a remote sensing-based assessment in both the Cauvery and Vennar command areas, downstream from the Grand Anicut canal (Figure 1, Map C), which will be modernized in stages over the coming years. This covers a total area of 5,420 km^2.

18. Due to the current lack of in situ data to describe canal flows or irrigation water delivery, very little information is available to understand where there are problems with water delivery across the command areas, and to assist in spatial targeting of irrigation investments within the CDZ.

19. While a Decision Support System (DSS) is proposed to be developed for improved decision making by providing real-time information on water levels and flows in the main channels, and thus ultimately to improve irrigation water distribution to achieve equity in delivery, it is not yet fat a stage where it can be used in the preparation of Project 2. The analysis of remote sensing data presents a relatively low-cost opportunity to fill this information gap.

20. The objective of the study is thus to define and undertake a remote sensing-based assessment which can be used by the Project Technical Advisory Consultants (PTAC) to

identify which canals and locations should be included in Project 2, and thus to prioritize areas for investment.

21. Various irrigation performance indicators can be derived at scales by the integration of remote sensing and weather data into surface energy balance models. Those indicators can help in identifying potential issues as well as to guide potential interventions to improve agricultural productivity and beneficial water consumption over the command areas. Following discussions with ADB, two indicators were selected:

(i) Spatiotemporal variability in biomass production to assist in the identification of areas of very low production;
(ii) Relative water deficits, an indicator to scale the actual crop water stress with reference to maximum (i.e. unstressed) crop evapotranspiration (Steduto et. al., 2012).

22. IHE Delft and IWMI have proposed to use the pySEBAL approach (detailed in Mul et al., 2020) for analyses at the irrigation command scale to derive the data on biomass production and ETa; this approach uses satellite images and weather data to map agricultural water consumption (ETa) and biomass production. Two additional outputs are provided; crop yields, and Crop Water Productivity (CWP). This approach, and the pySEBAL tool in particular, have been developed through, and widely used in other similar studies funded by ADB and implemented by IHE Delft and IWMI.

23. PySEBAL processes the surface energy balance and plant growth at landscape level with a grid of 30 m independent of crop type information. The ETa and biomass production of individual crops can be derived without any a priori information on the type of crop and type of soil. A crop map is required, however, for making crop specific production analysis such as for scheme specific crop yields and for crop water productivity.

24. As the request for information from ADB and the PTAC concerns the delivery of water and the timing and spatial patterns of any issues related to this, as well as information on biomass production, the scope of the study was defined as follows:

a. Quantification of the accumulated biomass production during an annual irrigation season;
b. An analysis of ET deficits over the same time period as a diagnostic tool to identify spatial and temporal variations in water delivery across the command areas.

25. The time period for the analysis was initially identified as the irrigated rice growing seasons during the 12 months from January to December 2018, although it was noted during the inception phase that this may vary depending on the availability of cloud free images.

26. The study began in September 2019, and it was agreed that where possible a rapid assessment would be undertaken to align with Project Preparation for Phase 2; this required presentation of initial results in November 2019. Following the discussions presented below, the analysis was performed for the year 2017.

IV. WATER DEFICIT ASSESSMENT

A. Background: Site Description

27. The Cauvery river is among the most important rivers in India. It is about 802 km long and with a basin area covering parts of Karnataka (34,273 km^2), Tamil Nadu (43,856 km^2) and Kerala (2,866 km^2). Tamil Nadu is the largest beneficiary of the Cauvery River as it supports almost 12,000 km^2 cultivable land in the state, most of which is located in the CDZ. The CDZ covers an area of more than 14,000 km^2, of which around 4,860 km^2 is irrigated from the canals and rivers network of the Grand Anicut. The Cauvery River irrigation water to the CDZ is supplied from the Grand Anicut via the Grand Anicut Canal network of 29,881 distribution canals which have a total length of about 22,400 km (PTAC 2018).

28. On its path towards the Bay of Bengal the Cauvery river downstream from the Grand Anicut divides into two rivers referred to as the Cauvery and Vennar, both of which provide irrigation water supply to the entire CDZ with their network of streams (Figure 1). The Grand Anicut is the dam that supplies water into the network of numerous canals in the Cauvery and Vennar portions of the CDZ. The Smaller Cauvery and the Vennar rivers in CDZ not only irrigate the agricultural lands but also provide domestic water to many cities in Tamil Nadu.

29. The irrigation and drainage systems in the Cauvery and Vennar command areas were adapted from the natural drainage systems a long time ago (particularly in the delta). These have typically only received essential maintenance over the past few decades, while over the last decade the situation has deteriorated further due to competing demands of various stakeholders and a changing climate. As a result, the distribution of surface water is inefficient and inequitable and tail end farmers do not receive adequate and reliable surface water supplies (PTAC 2018).

30. The CDZ is predominantly a rice-growing region. With some of the largest areas of agricultural land in the State, it is a significant contributor to the total national agricultural output. However, the Cauvery and Vennar command areas within the CDZ suffer from water shortages. Within these command areas, the availability of water resources is dependent upon surface water from the rivers.

31. Average annual rainfall in the greater Cauvery basin is more than 1389 mm/year, of which 56% (789 mm) falls during the Southwest monsoon, and 28% (386 mm) during the Northeast monsoon (Sushant et al., 2015). Within the basin, the CDZ lies in a marginally semi-arid region with average annual rainfall of around 1200 mm/year, and the availability of water resources is limited and highly variable. Most of the upstream areas and a large portion of the greater Cauvery river basin (outside the CDZ) receive rainfall during the southwest monsoon season (June – September). However, the CDZ receives the major portion of rainfall during the northeast monsoon season (October – November/December).

32. Figure 2 shows the rainfall distribution over the study area. In the CDZ, January to June are mostly dry months and August to December are mostly wet months. In 2017, the rainfall distribution indicates that November was the wettest month.

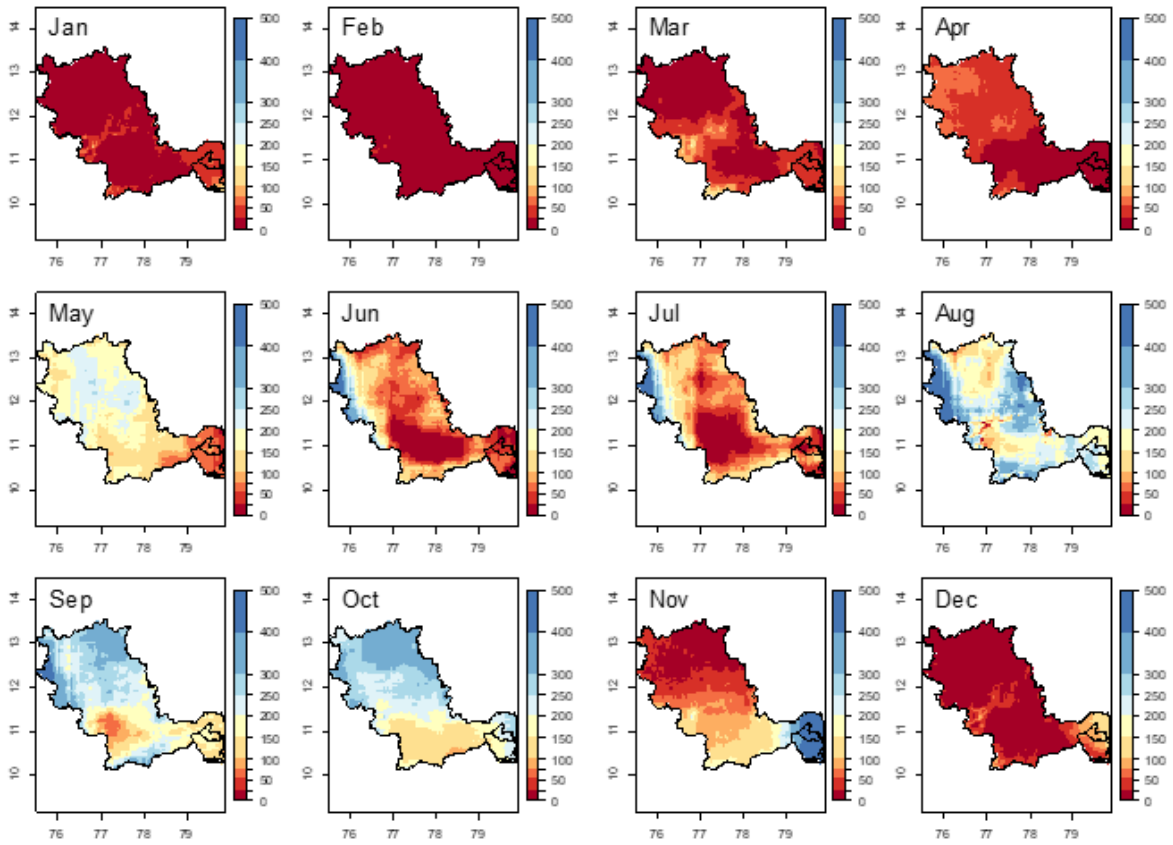

Figure 2: Spatial distribution of rainfall in the greater Cauvery basin (above) and in the Cauvery Delta Zone (below). Failure of rains in greater Cauvery during June-July months of 2017 the year of the study - led to delay in the release of irrigation water to the CDZ. Extreme dryness in the Vennar subbasin area during December 2017 resulted in high water deficit towards the end of Samba season (Image Source: CHIRPS data, Funk et al., 2015).

33. Rice paddy is the major crop grown in the CDZ region during both the pre-monsoon (April – July) and the monsoon seasons (August – December). Other crops such as Maize, Sugarcane, Gingelly (Sesame) and, a variety of vegetables are also grown during the pre-monsoon period, and pulses such as black gram and green gram (Mung Beans) are grown after rice to utilize residual soil moisture from the monsoon (Kannan et al., 2011). The three main cropping seasons in the districts covering CDZ are summarized in Table 1.

34. The rice paddy crop is grown during April to July (Kar/Karuvai/Sornavari season) and August to December (Samba/Thaladi/Pishanam season). It is frequently the case that the Karuvai crop experiences intermittent drought due to lower water availability and higher evapotranspiration demand (Geetalakshmi et al., 2011). Moreover, water scarcity is common in the delta when compared to the head and middle regions in the greater Cauvery basin. Table 2 shows the area under rice paddy irrigation in the districts located within the CDZ.

35. The major irrigation season is the Samba/Thaladi/Pishanam (Table 2) when irrigated rice is cultivated during August to November/December in over 90% of the irrigation command area. A small amount of irrigated rice is grown in the dry months (December to March), mostly cultivated using groundwater. In the regions closer to the coast (the extreme southeast of the command areas in Figure 1), water for irrigation is mostly extracted from groundwater sources through pumps or open wells. The abstraction of groundwater is resulting in declining groundwater levels and salinity intrusion (Ramkumar et al., 2010). Since Samba season covers up to 85% of the total irrigated area, we focus our study and analysis on the samba season.

Table 1: Cropping seasons within CDZ districts (Source: SCRT, 2012).

No	District	Kar/Karuvai/ Sornavari	Samba/Thaladi/ Pishanam	Navarai/Kodai
1	Thanjavur	April – August	August – December	January – April
2	Thiruvavur	May – August	August – December	January – April
3	Nagapattinam	June – October	October – January	January – April
4	Ariyalur	June – October	October – January	January – April
5	Cuddalore	May – August/September	August – December	January – April

Note. Major areas under Ariyalur and Cuddalore fall outside the CDZ; Data are not available Karaikal which falls within CDZ is under Pondicherry state.

Table 2: Area under irrigated rice paddy in the districts covering the CDZ (Source: SCRT, 2012)

No	District	Kar/Karuvai/ Sornavari (April – July)	Samba/Thaladi/ Pishanam (August - December/January)	Navarai/Kodai (December – March)	Total area (ha)
1	Thanjavur	23,083	119,103	4,773	146,959
2	Thiruvavur	12,775	142,888	3241	158,904
3	Nagapattinam	13,553	112,845	950	127,348
4	Ariyalur	728	12,473	365	13,566
5	Cuddalore	18,784	86,729	6,445	111,958
	Total	68,923	474,038	15,774	558,735

Note. Major areas under Ariyalur and Cuddalore fall outside the CDZ.

B. Summary of the approach

36. Water Productivity (WP) is a performance indicator that can be used for monitoring, evaluating, and diagnosing agricultural water management practices; the concept is described in detail in the technical manual developed through this project (Mul et al., 2020).

37. WP focuses on the consumed water; the water productivity of agricultural activities can be quantified on the basis of crop yield harvested and net water consumed. Remote Sensing (RS) based assessment of WP focuses on actual evapotranspiration (ETa) to estimate net water consumption. IHE Delft and IWMI, through discussions with ADB, have agreed to use the pySEBAL tool for this purpose.

38. pySEBAL is a library of python codes used to implement the Surface Energy Balance Model (SEBAL) from spatial data including spectral reflectances, climatic parameters, and altitude as inputs to estimate the surface energy balance components (Bastiaanssen et al., 1998a, 1998b). The outputs include parameters related to the energy balance, vegetation and biomass, the ET, and WP.

1. Methodology: pySEBAL

39. SEBAL is a single-source model that uses visible, near-infrared and thermal infrared data collected mainly by sensors on board earth observation satellites (Bastiaanssen, 2000). SEBAL has the advantage over conventional methods of estimating ET from crop coefficient curves or vegetation indices in that crop development stages do not need to be known, nor do specific crop types.

40. pySEBAL, developed by IHE Delft, is based on the use of RS and meteorological data to estimate actual and potential evapotranspiration rates along with other energy exchanges between the land and atmosphere.

2. Data inputs

41. A full specification of the data requirements for the pySEBAL model are detailed in Mul et al. (2020); only data which are specific to the current analysis are provided here.

42. Spectral radiances in the visible, infra-red and thermal range of the electromagnetic spectrum are the main input to the SEBAL model. Data from the Landsat satellites are typically used for this purpose; the high spatial resolution (30m) of the data provides sufficient detail to characterize the spatial patterns of biomass production and water deficits across the command area, and the revisit time of 16 days can, under cloud free conditions, provide sufficient coverage of an irrigation season.

43. Images from two consecutive rows are required to cover the entire command area of the Cauvery-Vennar subbasins (path 142 row 53, and path 142 row 52). The data are available for download at no cost from the USGS Earth Explorer website (https://earthexplorer.usgs.gov/).

44. A total of 19 images were downloaded for the year 2018. Details of these along with cloud cover percentages are provided in Table 3. This indicates that only 5 images (covering 4 months – January, May, July and September) out of the 19 images acquired had less than 30% cloud cover over the command area. The remainder of the acquisitions (14 out 19) could not be used due to the high levels of cloud cover. As this does not provide sufficient coverage of the irrigation season, analysis for 2018 was not feasible and images were assessed and acquired for 2017 instead (Table 4).

Table 3: Landsat 8 Image availability and cloud cover (2018).

Acquisition Date (2018)	**Cloud Cover (%)**
January 07	5
January 23	62
February 08	61
February 24	71
March 12	84
March 28	51
April 13	97
April 29	75
May 15	100
May 31	29
Jun 16	46
July 02	13
July 18	97
September 04	26
September 20	20
October 22	98
November 07	91
December 09	76
December 25	86

Table 4: Landsat 7 (denoted with a *) and Landsat 8 image availability and cloud cover (2017).

Acquisition Date (2017)	**Cloud Cover (%)**
January 20	11
February 13*	45
March 25	0
April 02*	16
April 10	10
April 18*	3
April 26	3
May 28	32
June 05*	7
June 13	55
June 29	1
July 15	12
July 31	4
August 08*	0
September 01	23
October 03	21
October 19	1
November 20	28
December 30*	26

45. For the year 2017 a total of 13 cloud-free acquisitions are available from the Landsat 8 sensor. The months where cloud-free images were not available from Landsat 8, gaps were filled with images from the Landsat 7 sensor. A total of 6 Landsat 7 images covering 3 months (February, August and December) were acquired for this purpose. Landsat 7 images have missing data due to a scan line correction (referred to as "SLC-off") error. The Landsat Toolbox in ArcGIS was used to fill in the data missing due to this error.

46. The final set of images used in the analysis and the corresponding sensors for each acquisition are shown in Table 5.

Table 5: 2017 Landsat images selected for analysis

Month	**Acquisition Date (DD/MM/YY)**	**Sensor**
January	20/01/17	Landsat 8
February	13/02/17	Landsat 7
March	25/03/17	Landsat 8
April	10/04/17 and 26/04/17	Landsat 8
May	28/05/17	Landsat 8
June	13/06/17 and 29/06/17	Landsat 8
July	15/07/17 and 31/07/17	Landsat 8
August	08/08/17	Landsat 7
September	01/09/17	Landsat 8
October	03/10/17 and 19/10/17	Landsat 8
November	20/11/17	Landsat 8
December	30/12/17	Landsat 7

47. A time-series of meteorological parameters at the time of satellite data acquisition (instantaneous) and the 24-hour average representing the day of acquisition are required to implement the pySEBAL model; these are needed to calculate the soil water balance and Penman Monteith Standard Reference Evapotranspiration (see Mul et al. (2020) for full details). Ideally, on-site weather station data would serve this purpose. As these were not available either from the PTAC team or the IWMI India Office, and could not be obtained in the short time frame of project implementation, they were obtained from a global weather dataset instead.

48. Instantaneous (hourly) and daily average data from the NASA Global Land Data Assimilation System (GLDAS v2.1; https://ldas.gsfc.nasa.gov/gldas) were acquired for the command areas and used as input to the pySEBAL model. GLDAS is an assimilated global data product from satellite and ground-based observations, with data available at 0.25-degree spatial resolution and at 3 hourly intervals. The parameters used are listed in Table 6.

Table 6: Meteorological data inputs to the PySEBAL model

Parameter	Symbols	Unit
Downward shortwave radiation	SWdown	W/m^2
Wind speed	Ws	m/s
Air temperature	Tair	°C
Pressure	P	Mb
Relative humidity	Rh	%

49. A Land use/land cover (LULC) map or a map depicting the location of irrigated areas, or boundaries of the irrigation system, is needed to ensure that the analysis is limited to the relevant areas. As no recent or high resolution LULC map was available for the study area, a previously produced irrigated area map (IWMI 2013) was used to identify the areas of irrigated single, double and continuous/three cropping regions (Figure 3) for further analysis. While the data are from several years ago (2012) a discussion with ADB confirmed that the cropping systems in the CDZ have been relatively static over this time.

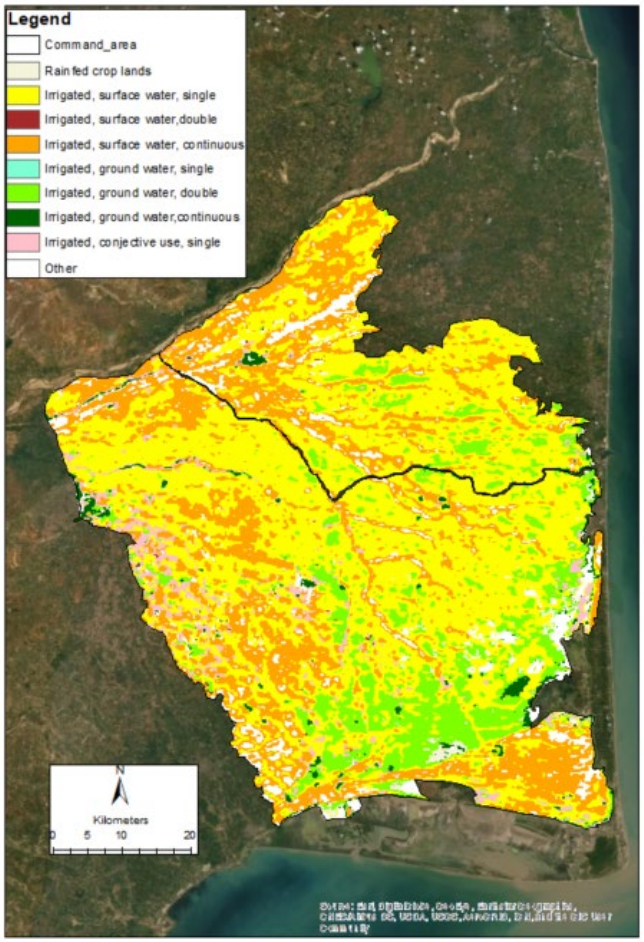

Figure 3: High spatial resolution iirrigated area map (Source: IWMI 2013).

50. Analysis of these data (Figure 3) indicates that nearly 93% of the command area is irrigated. Irrigated (surface water) single cropped systems occupy around 54% of the command area, followed by irrigated (surface water) continuous cropping systems, occupying around 30% (Table 7).

Table 7: Irrigated area statistics for the Cauvery and Vennar command areas obtained from IWMI 2013 Irrigated area map

	Cauvery Command Area (km^2)	Vennar Command Area (km^2)	Total Command Area (km^2)
Total Area (km^2)	1,266	3,352	4,619
Irrigated, surface water, single	54.2	49.8	51.0
Irrigated, surface water, double	0.1	0.1	0.1
Irrigated, surface water, continuous	31.0	23.5	25.6
Irrigated, groundwater, single	0.0	0.0	0.0
Irrigated, groundwater, double	6.7	13.4	11.6
Irrigated, groundwater, continuous	0.6	1.9	1.5
Irrigated, conjunctive use, single	1.0	4.9	3.9
Other	6.3	5.8	5.9

51. The map of irrigated areas (Figure 3 and Table 7) identifies different cropping systems (single, double and continuous) supplied by either surface water from the rivers or from groundwater sources. In this study we focused on analysing areas supplied by surface water.

52. Following the collection and preparation of the various input datasets, the pySEBAL model was implemented following the steps shown in Figure 4. The acquired Landsat 7 and 8 data were pre-processed to create cloud masked Top Of Atmosphere (TOA) reflectance. The pre-processing included conversion from Digital Number (DN) to TOA reflectance, cloud removal using the Quality Assessment (QA) band provided along with the data, and mosaicking the same image path tiles. These pre-processing steps (Steps 1 and 2, Figure 4) are performed inside pySEBAL.

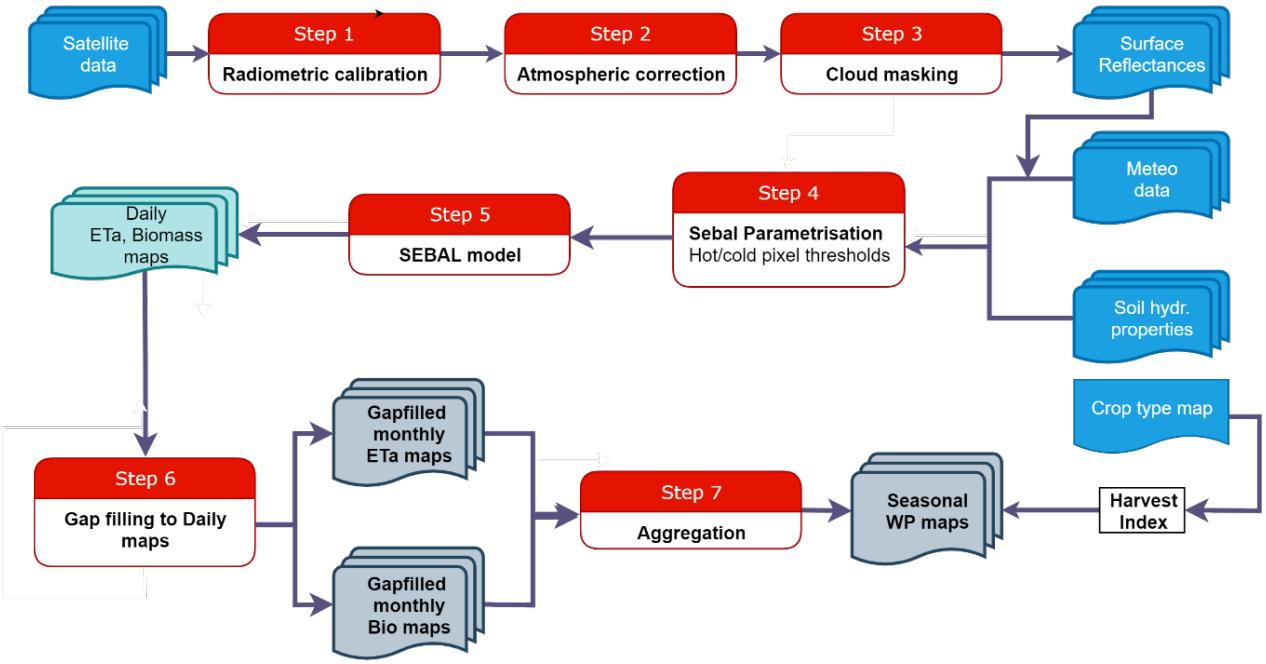

Figure 4: The pySEBAL methodological framework (Source: Mul et al., 2020).

3. Cloud masking and gap filling

53. The pySEBAL approach is dependent on the availability of cloud free optical satellite images of the land surface during the period of interest for the selected project sites. While the Landsat satellites data archive is one of the most useful data products to monitor the Earth's surface at a high spatial resolution, given the temporal coverage of 16-day, the degree and extent of cloud coverage is always a challenge and will vary from region to region. Due to the proximity to the coast and the monsoon climate, the Cauvery-Vennar command area shows a high degree of cloud cover throughout the year (see Table 3 and Table 4).

54. The images selected for analysis (Table 4) still contain cloud cover of varying amounts; the frequency of cloud cover is shown for each pixel within the Cauvery and Vennar command areas (Figure 5). Higher cloud cover can be seen closer to the coast, with a very high prevalence in the southeast delta region of the Vennar command area.

55. In the standard pySEBAL implementation, areas covered by clouds are identified, masked out and subsequently filled using a linear interpolation algorithm (Step 3, Figure 4). While this is a suitable approach for land cover classes which are relatively static between consecutive image dates (e.g. forests), using a linear interpolation algorithm can result in inaccurate estimation of ETa. This is due to the fact that the cloud-free image acquisition dates from the same Landsat sensor will be a minimum of 16 days apart, and frequently more in regions like Tamil Nadu where cloud cover is common during the cropping season. Moreover, some rain events may occur in between satellite images, the effects of which are not recorded in a subsequent image, and therefore those evaporation amounts are not fully accounted for. Hence, linear interpolation does not suitably capture the effect of vegetation growth following the last image and does not reflect for any antecedent soil moisture (Irmak et al., 2012).

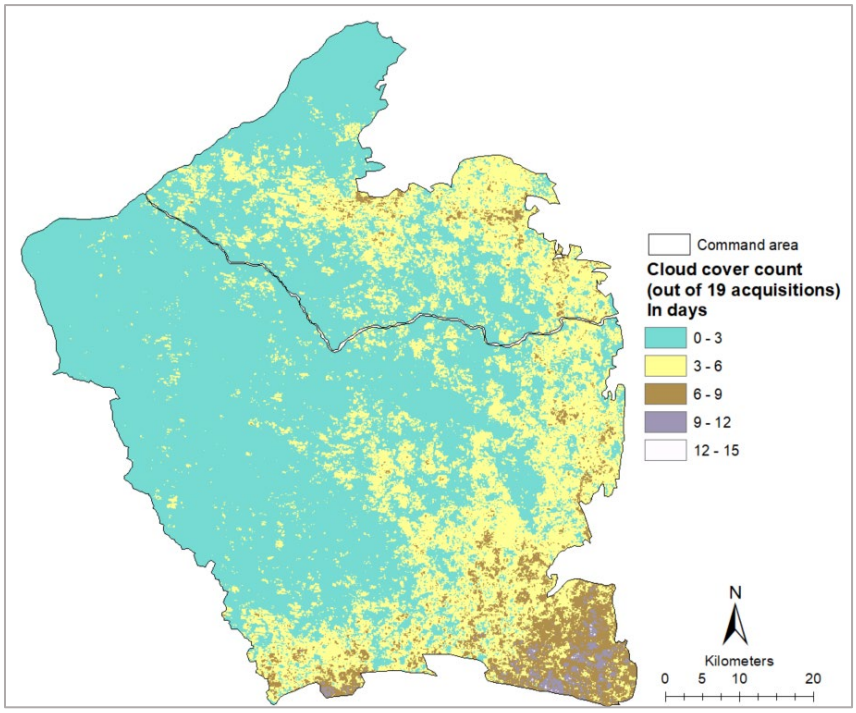

Figure 5: Landsat cloud cover statistics, 2017.

56. We therefore applied an approach to the crop coefficient ("Kc") image output from pySEBAL in order to fill gaps due to cloud cover; the approach uses the pySEBAL cloud mask image, and adds an extra processing step which aims to improve the already gap-filled Kc estimates from pySEBAL. The gaps in the Kc image following the cloud masking are filled using a linear, time-weighted interpolation of the Kc values from the previous image and the nearest following satellite image date which has a valid Kc estimate, adjusted for vegetation development. In gap filling procedure, the interpolated values for the clouded and cloud-shadowed areas are adjusted for differences in residual soil moisture between the image dates which occur as a result of heterogeneities in precipitation (for example localized showers) in inverse proportion to the Normalised Difference Vegetation Index (NDVI), and by adding an interpolated 'basal' Kc from the previous and following satellite image dates. The procedure is explained in detail in Irmak et al. (2012).

4. Water Deficit Analysis and Biomass production

57. The ET deficit is an essential performance parameter that is output from the pySEBAL approach. The ET deficit is calculated as the ratio of the reference evapotranspiration (ETref) which represents the water unlimited ET during crop development, and the actual (measured) ET (ETa). The ET deficit is a direct expression for any water shortage the crop is experiencing on a pixel by pixel basis, and it can help to assess (without any further information on canal flows) whether the crop has sufficient moisture in the root zone. This information is useful in understanding and interpreting irrigation performance across a command area.

58. Through discussions with, and request from ADB, the ET deficit was normalised (i.e. so that the values varied between 0 and 1, where 0 indicates no deficit and 1 indicates extreme deficit) and referred to as a "Relative Water Deficit" (RWD). The RWD was calculated

according to Equation 1, where ETa/ETref is the ratio of the actual ET (based on the satellite images and derived through the pySEBAL model) to reference evapotranspiration (see Mul et al., 2020 for full details).

$$RWD = (1 - \left(\frac{ETa}{ETref}\right))$$

Equation 1

59. The RWD is essentially a direct expression for water shortages experienced by the crop at a particular point during a cropping season (Jackson et al., 1981); assessment of the RWD can provide insights into deficit conditions (and thus water availability) across the command area for a particular crop (in this case rice), over a particular season (in this case the Samba season). The RWD often correlates with other biophysical parameters such as biomass and ETa. For example, regions with high RWD (high stress) translate to low crop biomass production, which in turn gives an indication of the areas where there are yield losses due to limited water supply.

60. The second parameter calculated from the remote sensing data is the Above Ground Biomass Production (AGBP). The calculation of AGBP, and the calculation of crop yield which is further derived from the AGBP, are primarily based on the relationship between the absorbed light and carbon assimilation by the plant. The AGBP is an output from the pySEBAL approach, and full details of the algorithm used to calculate this and related parameters can be found in Mul et al. (2020).

5. Crop Yields and Water Productivity

61. AGBP is an output from the pySEBAL approach. In order to calculate crop yields, the biomass maps are converted to yield maps using a Harvest Index (HI), which is typically established with field data. The relationship between biomass and grain yield for rice, for example, depends on many elements such as seeds, crop temperature, nutrient, and water stress. As field data was not collected and yields for the season and command areas studied were not readily available, we have identified a HI from other reports. Mohandas et al. (1993) reported HI as high as 0.7 in rice systems in the Cauvery river basin; Rajesh and Thanunathan (2003) reported a HI of 0.3 in the traditional rice varieties grown in the Cauvery river basin region; while Jaypriya and Porpavai (2019) reported a HI of 0.45 for different rice systems in Tamil Nadu. Based on the literature, we considered an average HI of 0.45 for this study to estimate yields. The yield is calculated as:

$$Yield = HI * AGBP$$

Equation 2

62. Finally, Crop Water Productivity (in kg/m^3) for the irrigated rice pixels in the command areas was calculated following Equation 3 where the water consumed is calculated as the total ETa over the growing season:

$$WP = \frac{Yield}{Water\ consumed}$$

Equation 3

C. Presentation of Results

63. The pySEBAL based Water Productivity analysis (encompassing the estimation of biomass production, crop yields, ETa, and water deficits) has been performed in this study to provide the information needed to guide the identification and prioritization of investments to improve the productive use of water through improved supply across the command areas.

1. Crop Water Consumption

64. The actual evapotranspiration (ETa) has been generated for the Samba season by integrating a time series of Landsat 7 and 8 images for the period August to December 2017, for the irrigated rice areas within the study area (Figure 6). The map of ETa reveals the level of water consumption as well as the spatial variability across the command area. Total seasonal ETa varies from around 200 mm to 850 mm with a mean value of 535 mm, which aligns with the range of normally observed values (Cai and Bastiaanssen, 2019).

65. High and systematic variations in ETa are observed for the rice system (Figure 6). Most of the northern part of the command area (including the majority of the Cauvery subbasin) shows high ETa (>600 mm) with isolated patches of lower values. In contrast, the irrigated areas within the Vennar subbasin demonstrates higher spatial variability in ETa, with highest values (>600 mm) in the northwest region, and lower values over large areas as well as a marked decline overall from northwest to southeast, towards the coast.

66. The histogram distribution of the ETa values for the command areas shown in Figure 6 is presented in Figure 7. The histogram shows a near-normal distribution with a mean of around 535 mm. The areas with lower ETa are the regions experiencing water stress and the areas with higher ETa correspond to areas with higher water availability. It should be noted that in some locations within the command area the Samba season may extend into January; this means that the season total ETa as calculated (August to December) may be slightly underestimated.

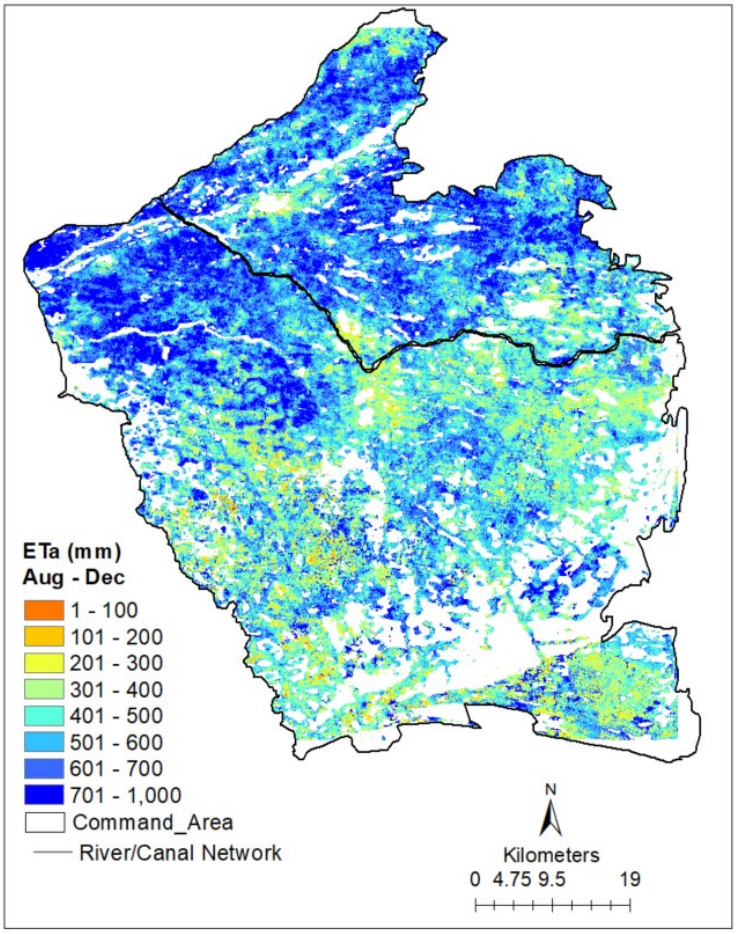

Figure 6: Samba seasonal total ETa for the Cauvery and Vennar command areas.

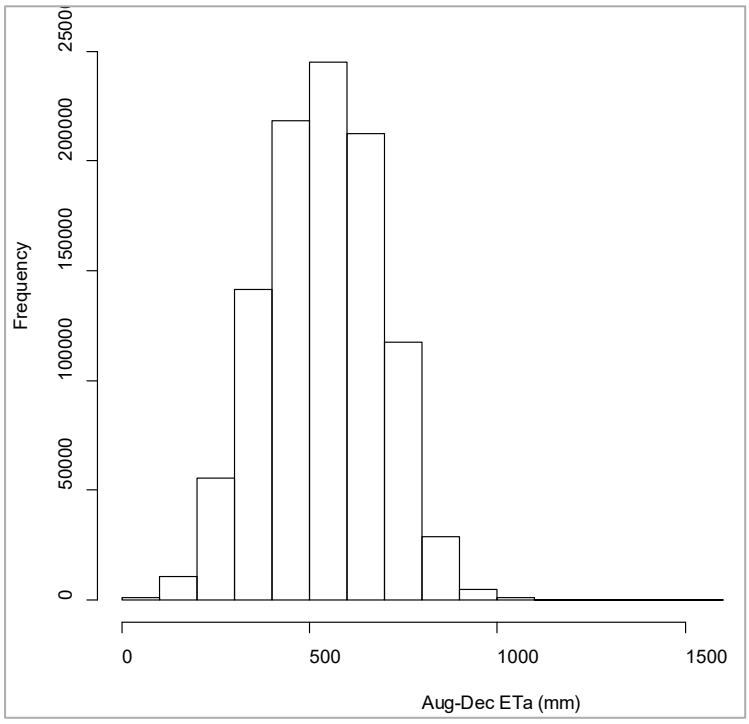

Figure 7: Distribution of 2017 Samba seasonal total ETa values for the Cauvery and Vennar command areas.

2. Relative Water Deficit

67. The mean monthly RWD estimates for the 2017 Samba season are presented in Figure 8. These results clearly indicate a higher deficit at the start of the season (in August), with the situation improving by the end of the season and a reduction in the total area experiencing deficits. In the Cauvery subbasin, the early season deficit was around 35% (i.e. 65% of the demand was being met), reducing to almost no deficit by the end of the season. Similarly, the Vennar sub-basin experienced up to 40% deficit during the beginning of the season. This could be due to the combined effect of failure of rains in the early season (June-July, see Figure 2) and as a greater area left as fallow as a result of low water availability early in the season). In contrast, higher deficits (up to 20%) still persisted towards the end of the season, especially in the command areas in the Vennar subbasin (irrigated areas along the Thanjavur – Thiruvavur district boundary). During December 2017, this region experienced higher dryness when compared to other regions in the CDZ. Extreme dryness towards the end of the season (see Figure 2) may have resulted in up to 40% irrigation water deficit in this region.

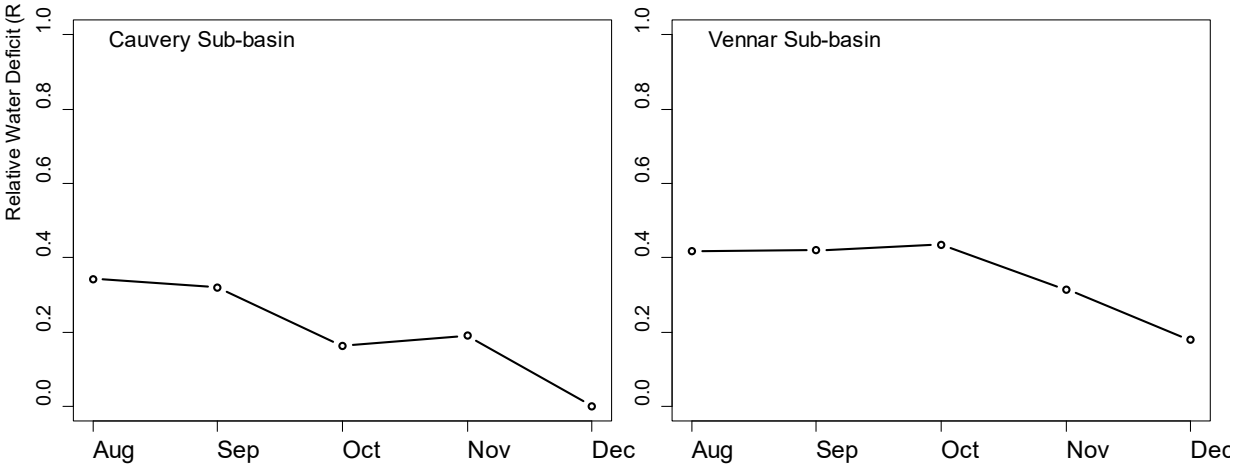

Figure 8: Temporal variability in mean RWD across the irrigated areas in the Cauvery and Vennar Basins during 2017 Samba season.

68. The higher water deficit at the beginning of the growing season indicates the inability of the irrigation infrastructure to meet the water demand at the start of the growing season. A decline in water deficit at the end of growing season could possibly be attributed to rainfall. Figure 9 shows that approximately 500 mm of rainfall was received during November 2017. Moreover, the smaller Cauvery and Vennar rivers are dual purpose rivers, they also serve as drainage channels in the CDZ. Hence, water demand at peak growing season would have been met by irrigation water supplied, and towards the end of season either directly from rainfall events or indirectly from drainage water.

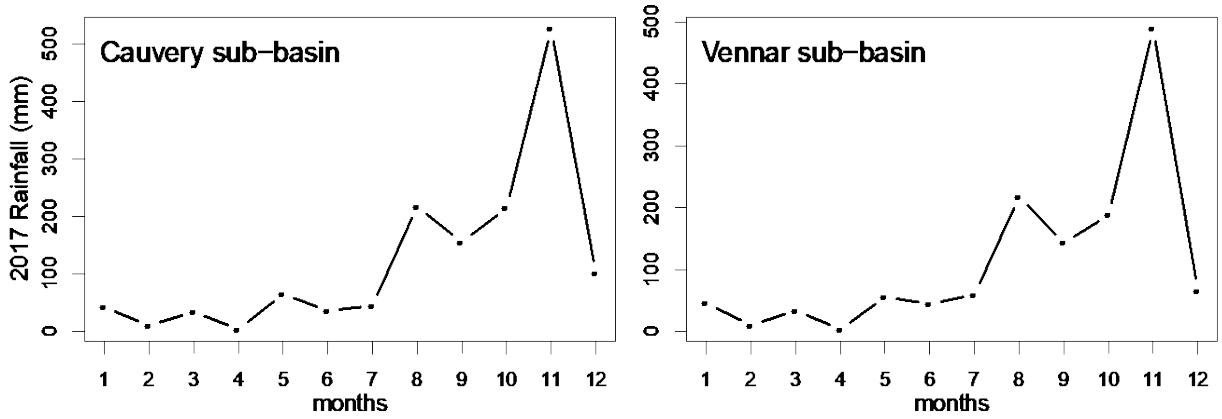

Figure 9: Average monthly rainfall during 2017 in CDZ.

69. In order to interpret the spatial distribution of different levels of water deficits and their persistence across the command areas, maps showing the percentage of the Samba 2017 season during which a pixel location experienced different levels of water deficits are displayed in Figure 10. The colour indicates the percentage of time a specific level of deficit was experienced.

70. For example, Figure 10a shows the percentage of the season each location experienced a deficit of 0.1 or higher. In the blue areas water deficits were only experience occasionally during the 2017 Samba season; in comparison the red areas experienced a water deficit persistently, during most of the season.

71. The second map, Figure 10b, presents the same information for a higher level of deficit (i.e. RWD of 0.3 or greater). The higher levels of deficit are more persistent in the southern half of the map, and more so in the Vennar command areas (the red and yellow areas), compared to the Cauvery command areas the blue areas).

72. The third map, Figure 10c shows the proportion of time even higher levels of deficit are experienced (i.e. RWD greater than or equal to 0.5). It is evident in this map that there are certain locations where the high levels of deficit are experienced over longer periods of the season (the red and yellow areas).

73. As the level of deficit examined changes across the maps shown in Figure 10, going from all levels of deficit in the left hand map (Figure 10a) to focusing on areas of moderate deficit in the middle map (Figure 10b), to focusing on areas of high deficit in the right map (Figure 9c), the proportion of the Samba 2017 season during which the particular deficit level is experienced decreases.

74. A marked spatial trend is evident between the northern and the southern parts of the map; in particular, the moderate (Figure 10b) to high (Figure 10c) deficits are more persistent in the south-eastern section of the Cauvery command area, as well as in an isolated section in the south-eastern part of the Vennar command areas.

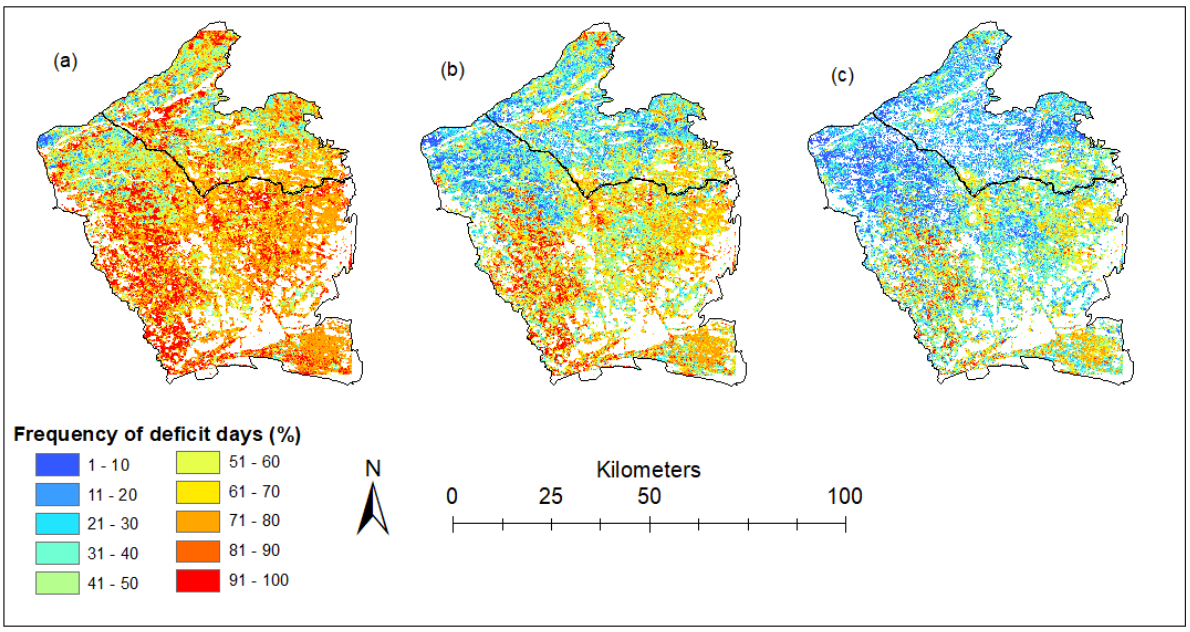

Figure 10: The different colours show the percentage of the 2017 Samba season during which different levels of water deficits are observed in the Cauvery and Vennar command areas. Figure a shows levels of RWD greater than or equal to 0.1; Figure b shows levels of RWD greater than or equal to 0.3; Figure c shows levels of RWD greater than or equal to 0.5.

3. Biomass production and yield estimation

75. The average AGBP mapped for the paddy rice area is 11.6 tons/ha (Figure 11). Lower than average values are mostly located a further distance away from the canal network, which is indicative of the disparity in the water distribution system. As would be expected, higher biomass production and AGBP values are located in areas which are closer to the irrigation channels and in the upstream portion of the command areas. Overall, within the Vennar command areas, mean season AGBP estimates are higher than the average measure for the study area.

76. The average yield across the command areas was found to be 6 t/ha. This estimate and the range shown in Figure 12: Rice yields in the Cauvery and *Vennar command areas estimated for 2017 Samba season.* is in line with yields reported in the literature; Geethalakshmi et al. (2011) reported that grain yield in the rice systems in the Cauvery basin varied from 3.5 t/ha to 7.3 t/ha, and Parthipan et al. (2013) reported that rice yield varies widely from 2 t/ha to almost 8 t/ha.

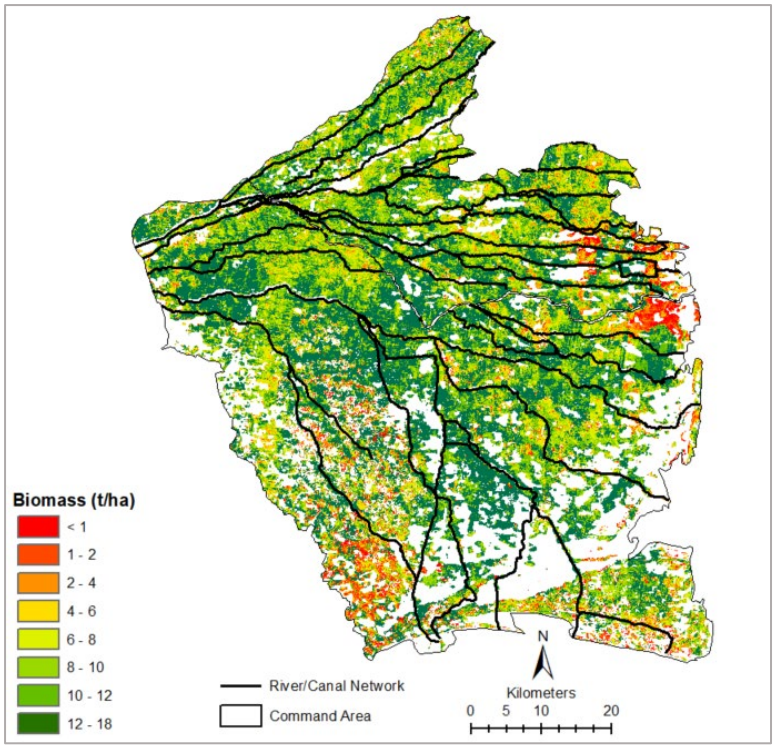

Figure 11: Accumulated biomass (kg/ha) modelled using pySEBAL for the 2017 Samba season (Aug-Dec) over the Cauvery and Vennar command areas. :

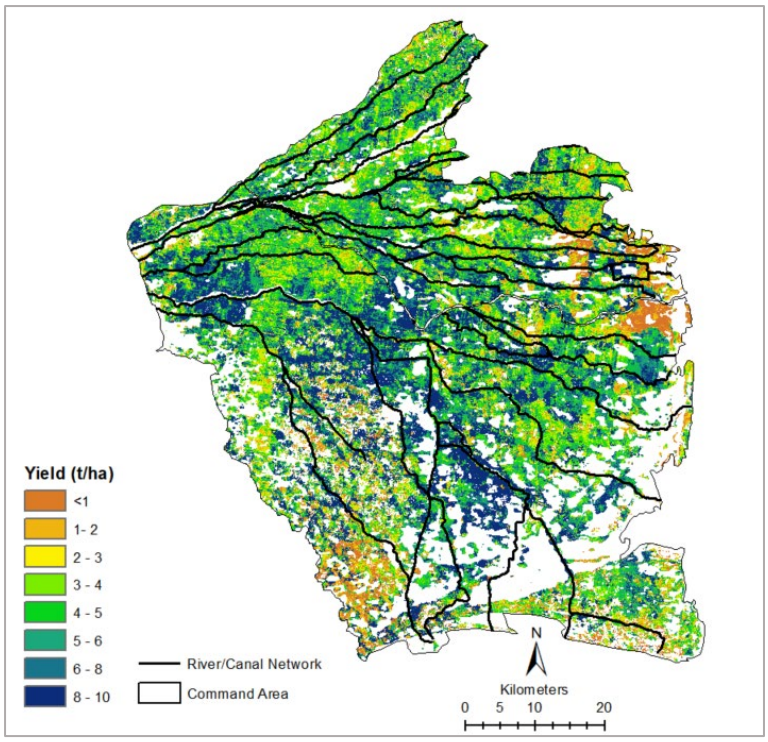

Figure 12: Rice yields in the Cauvery and Vennar command areas estimated for 2017 Samba season.

4. Crop Water Productivity

77. A very high variability and a distinct spatial pattern is evident in the CWP estimates over the irrigation command area (Figure *13*), with the Vennar indicating slightly higher values than the Cauvery.

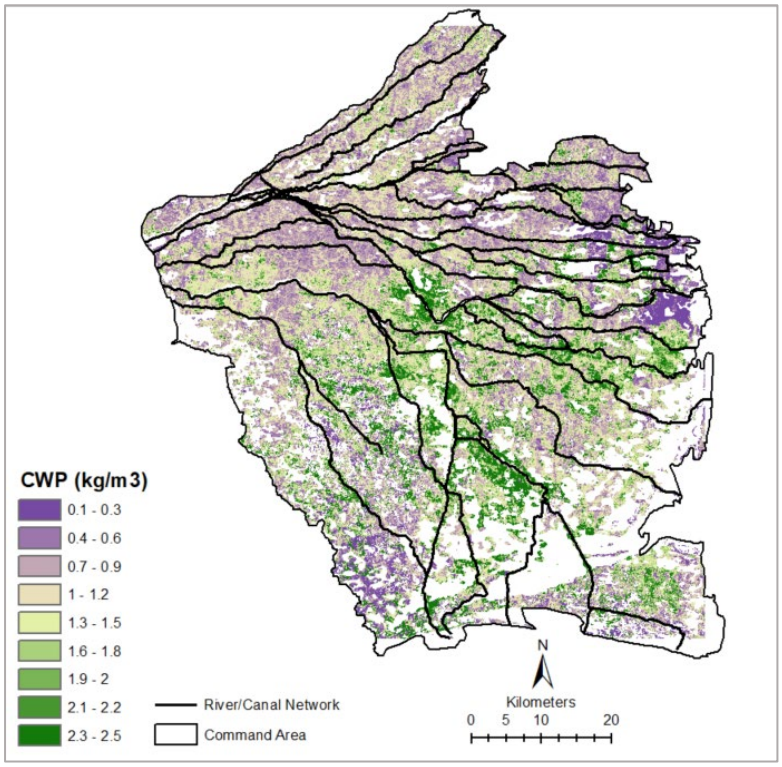

Figure 13: Crop water productivity for the Cauvery and Vennar commands during the 2017 Samba season.

5. Analysis of factors contributing to variations in AGBP

78. It would be expected that agricultural areas closer to the main river or canal network should show lower water deficit conditions and higher biomass production due to higher water availability; while agricultural areas that are far away from the river or canal network, often show higher water deficit conditions and lower biomass production due to lower water availability. In order to assess this, four different buffer zones were calculated from the river/canal network; <1km, 1-2km, 2-5 km and 5-10 km from the canal.

79. For each buffer zone, we classified biomass into below average, average and above average biomass classes based on the Mean (11.6 t/ha) and SD (6.85 t/ha) of the image. Results displayed in Table 8 and Figure 14 confirm that irrigated areas which are located closer to the canals show smaller area under below average biomass. As we move away from the canals, the area under below average biomass slowly increases. Beyond a distance of 5 km from the canal, we found that the area under below average biomass doubles.

Table 8. Percent area under below average biomass, average biomass and above average biomass summarized by distance from the stream zones.

Distance	Below Avg [< = Mean–SD]	Avg [Mean±SD]	Above Avg [> Mean+SD]
0-1	9.5	78.6	11.9
1-2	10.0	77.7	12.3
2-5	11.7	73.4	14.8
5-10	21.5	67.9	10.6

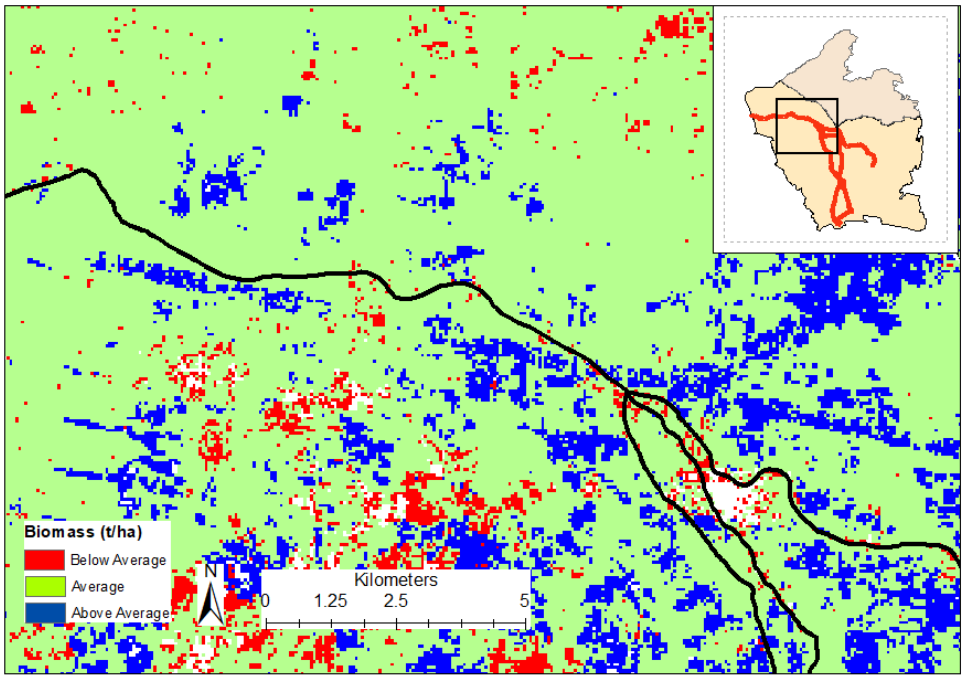

Figure 14: Illustration of biomass and distance from the Vennar river. A majority of irrigated areas show average biomass (mean±1SD) and several pockets closer to the river (black line) show above average biomass (>19 t/ha) and areas with below average (mean – 1SD) biomass (< 4 t/ha) are mostly seen farther from the river/canal.

80. Water abstraction from /canals within an irrigation command area is typically higher near the headwater location where water enters the system and is available for agricultural use. Further down the canal towards the tail end, the water availability decreases due to higher abstraction in the upstream area. Analysis of the canal length was performed to understand this occurrence in the study area.

81. In order to achieve this, the canals were coded according to the length from the head water location (Figure *15*), varying from 0 (at the head regulator end) to 130 km (the longest canal length). Based on the canal length, the Vennar and Cauvery command area is divided into 5 zones, and the analysis performed based on these.

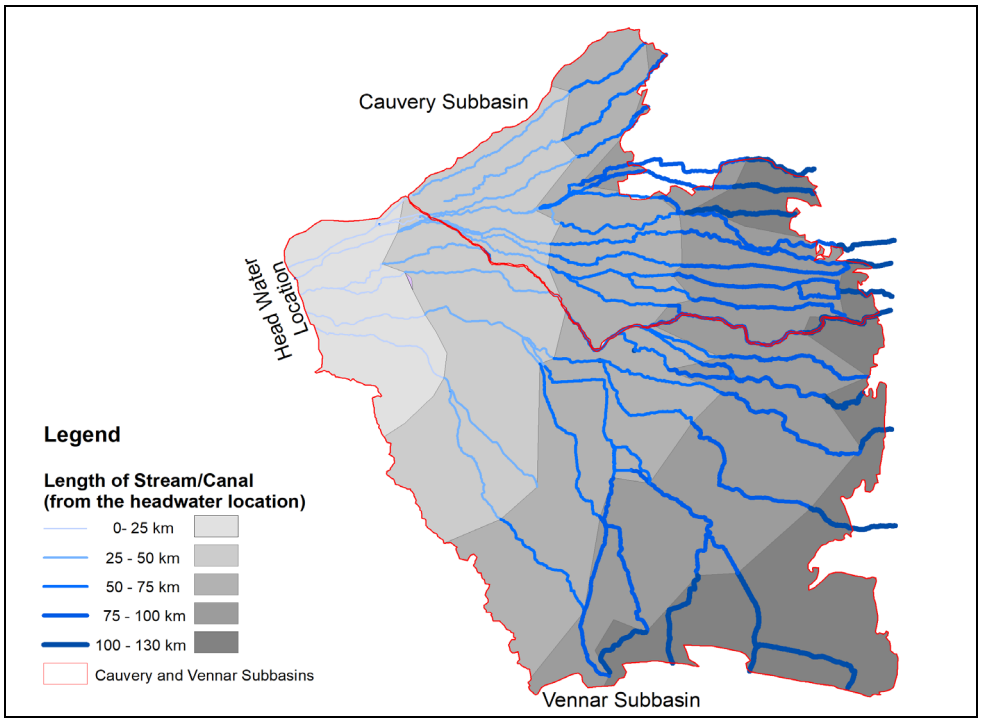

Figure 15: Length of irrigation canals in the Cauvery and Vennar subbasins

82. Results of the analysis are presented in the bar charts shown in Figure 16: Bar plots showing the impact of canal length on water deficit regions. The area under deficit slowly increases with longer canal length away from the head end of the canals.

83. In gravity systems water availability will also depends on elevation. Hence we compared deficit regions with eight different elevation zones (<0, 0-10, 10-20, 20-30, 30-40, 40-50, 50-60 and >60 m). The average AGBP (t/ha) is extracted for each elevation zone (Figure *18*).

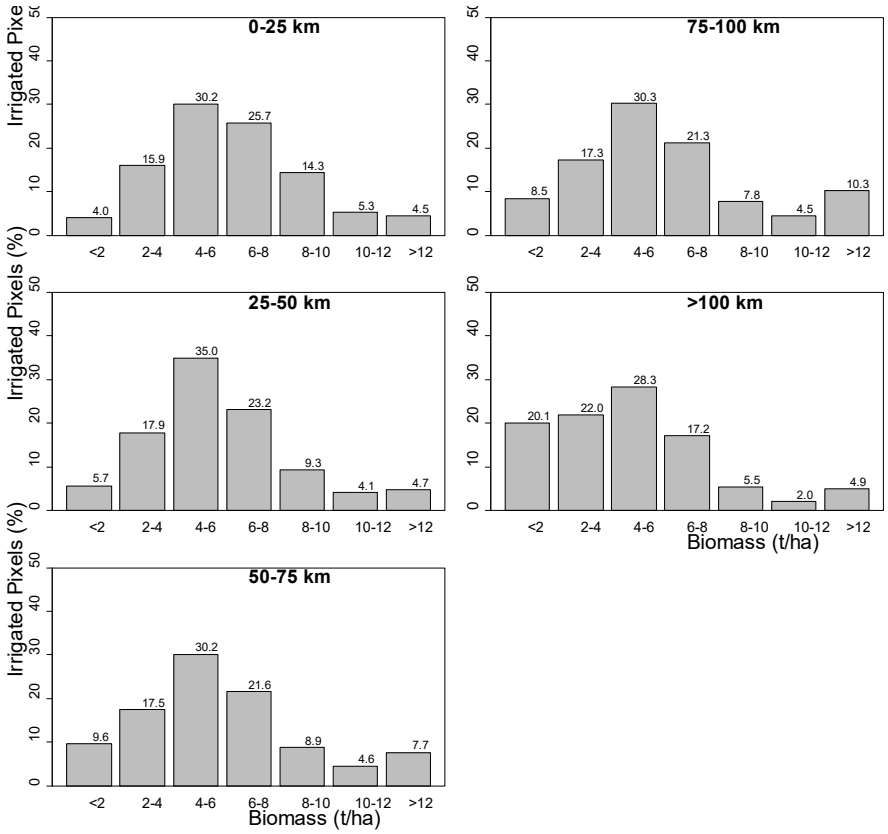

Figure 16: Bar plots showing the impact of canal length on water deficit regions. The area under deficit slowly increases with longer canal length away from the head end of the canals.

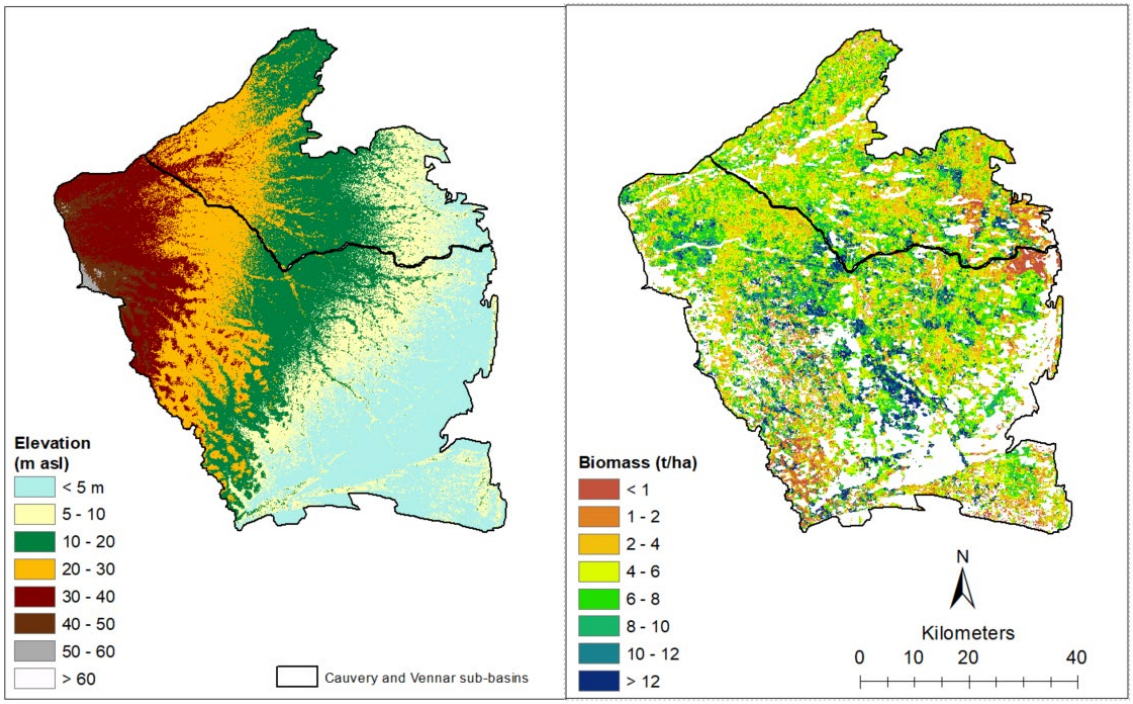

Figure 17: Elevation of the Cauvery and Vennar subbasins (left) and biomass production (right).

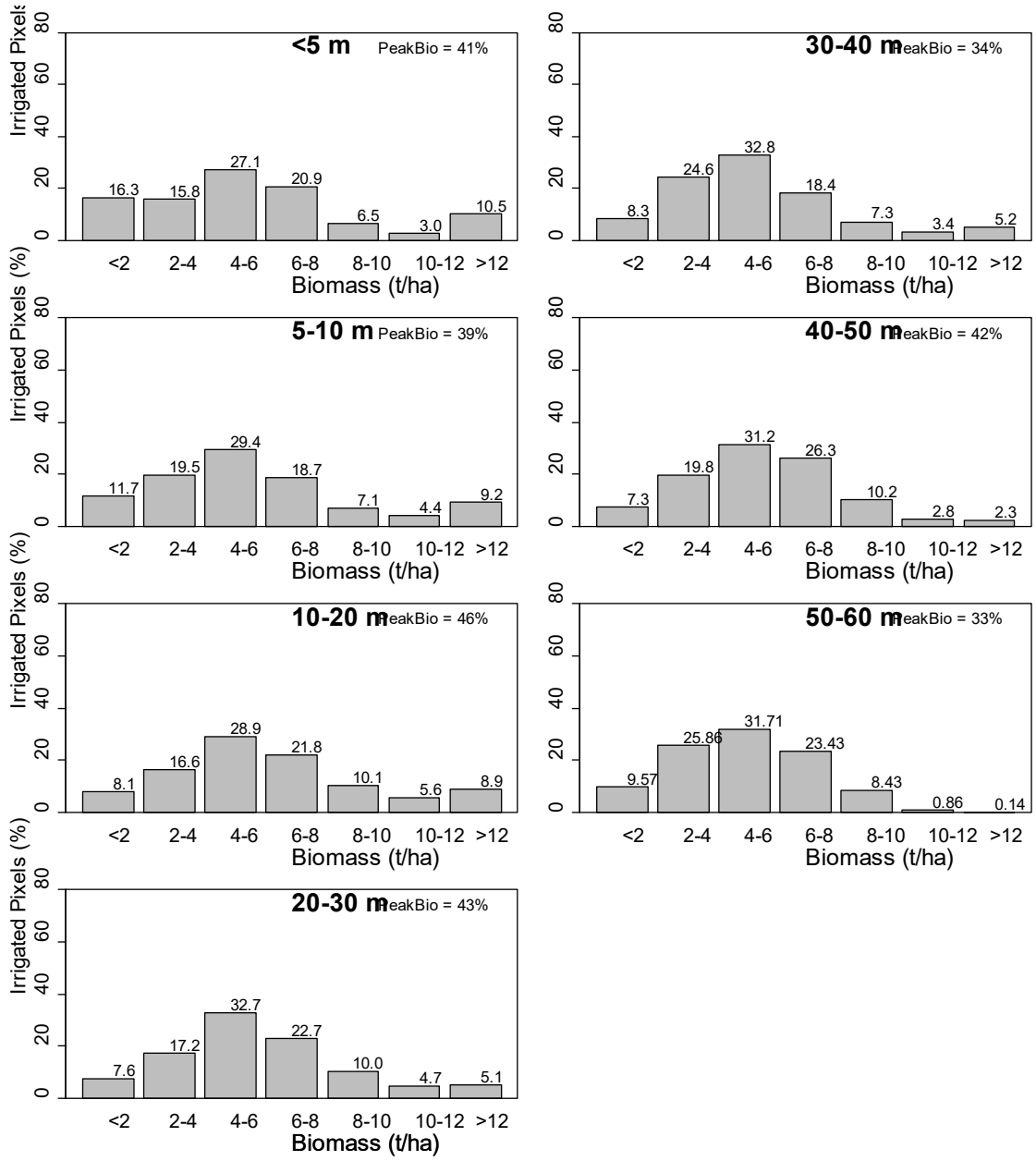

Figure 18: Histogram of biomass production across different elevation zones in the Cauvery and Vennar command areas.

84. The results (Figure *18*) demonstrate that there is high variability in AGBP produced in every elevation zone. From the histograms presented there is no substantial difference in distribution of pixels with a particular range of AGBP. Hence it can be understood that elevation does not have a substantial impact on the distribution of AGBP. This could be because of the lack of elevation range in the study area where elevation varies between 0 and 60 m.

85. We also investigated if a particular soil type influences the AGBP in the irrigation command area. We obtained the soil map from the TRTA team for the study region and simplified soil types into 10 broad classes as shown in Figure *19*. For each soil type, we summarized AGBP estimates to determine whether higher production values are correlated with particular soil types.

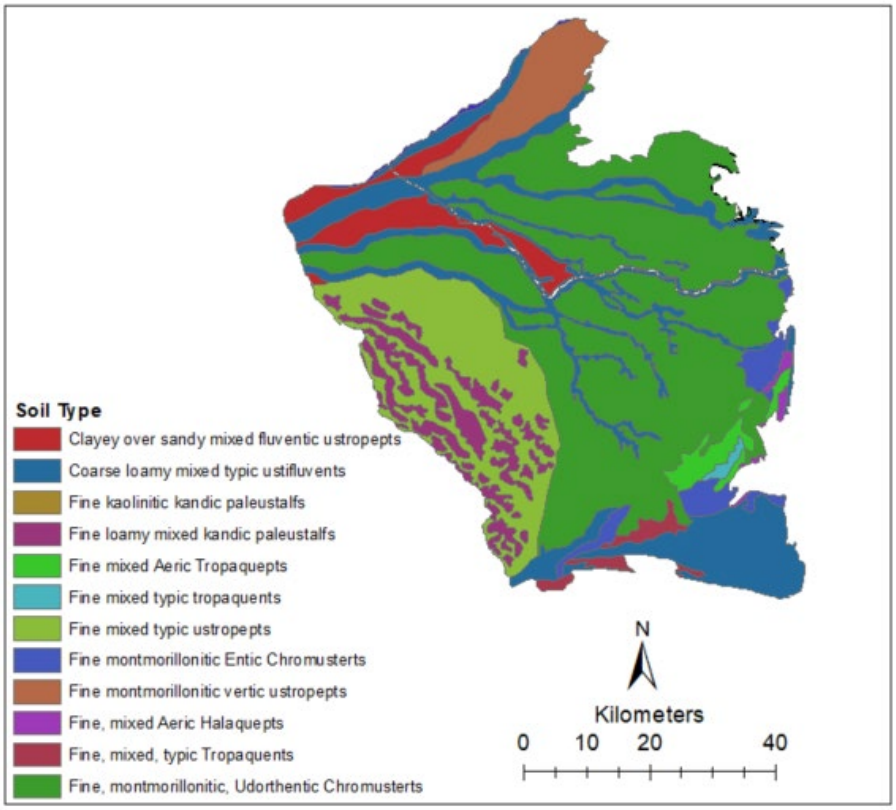

Figure 19: Map of soil type in the Cauvery and Vennar subbasins (Source: PTAC 2018).

86. Within the Cauvery and Vennar subbasins, there are three broad soil groups (Inceptisols, Alfisols and, Vertisols). Area under fine kaolinitic kandic paleustalf and fine, mixed, typic tropaquents was too small, we ignored them in our analysis.

87. Our results (Figure 20) indicate that biomass production is highly variable across soil types. The histogram plots show distribution of biomass under different biomass categories (on x-axis). A left skewed histogram (taller bars on the left side) indicates inability of that soil to produce high biomass. A right skewed histogram (taller bars towards right side) indicates a good soil for crop production. While most soils show normally distributed histograms (taller bars in the middle), indicates soil supporting average biomass production.

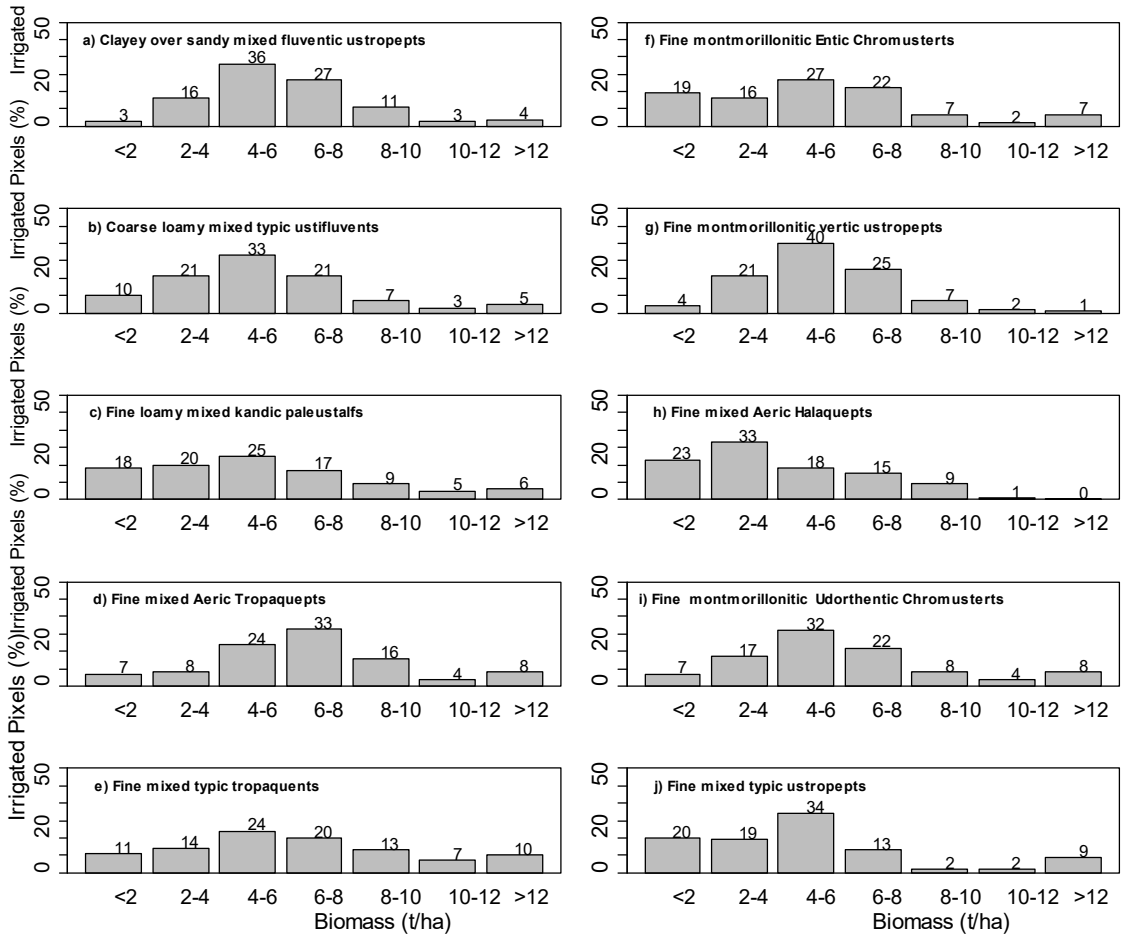

Figure 20: Distribution of 2017 Samba season AGBP for different soil types in the Cauvery and Vennar subbasins. The table 9 shows area under different biomass categories (below average, average and above average) for each soil type. While there is high variability in productivity (AGBP) within each group, fine mixed typic tropoquepts soil type showed largest percent of area under high biomass. Soil type “fine mixed aeric haplaquepts” showed largest percent of area under low biomass.

Table 9. Soil type and its performance of biomass production in irrigated rice systems during 2017 Samba in the CDZ. BA – below average; A – Average; BA – Below Avg.

No.	Soil order	Soil sub-order	Soil type	BA	A	AA
a	Inceptisols	Tropepts	Clayey over sandy mixed fluventic ustropepts	3	90	7
b	Inceptisols	Tropepts	Coarse loamy mixed typic ustifluvents	10	82	8
c	Alfisols	Ustalfs	Fine loamy mixed kandic paleustalfs	18	71	11
d	Inceptisols	Aquepts	Fine mixed aeric tropaquepts	7	81	12
e	Inceptisols	Aquepts	Fine mixed typic tropaquepts	11	71	17
f	Vertisols	Usterts	Fine montmorillonitic entic chromusterts	19	72	9
g	Inceptisols	Tropepts	Fine montmorillonitic vertic ustropepts	4	93	3
h	Inceptisols	Aquepts	Fine mixed aeric haplaquepts	23	75	1
i	Vertisols	Usterts	Fine montmorillonitic udorthentic chromsterts	7	79	14
j	Inceptisols	Tropepts	Fine mixed typic ustropepts	20	68	12

6. Analysis and interpretation of individual rivers

88. The Climate Adaptation in Vennar Subbasin in Cauvery Delta Project, tranche 2 will be carried out in 6 selected rivers, for which a preliminary analysis of the spatial variability was carried out which could provide insights to guide the investments and monitor post project impact. The six river segments include the Paminiyar, Manankondanara, Koriayar, Marakkakoraiyar, Vennar and Kaduvaiyar.

89. In order to provide this information river segments where water supply may be an issue as identified through areas of high water deficits have been located, along with the distribution of low production values along the various segments.

90. The location and distribution of water deficit areas for each of these selected river segments is displayed in Figure *21*. While the two smaller rivers (Manankondanar, and Marakkakoraiyar) generally persistent water deficits along the entire lengths of the channels during the 2017 Samba season, for the other 4 rivers it is possible to identify variations which may correspond to higher and lower performing segments over the Samba 2017 season, these are further elaborated in the paragraphs below. The identified higher and lower performing stretches are likely related to well-functioning and poorer functioning or damaged infrastructure or better and poorer operations. Focus on analysis of the infrastructure and operations of these stretches during the early stages of the detailed design might provide better insights into the best investments and measures to be taken as part of the CAVSCDP-project 2.

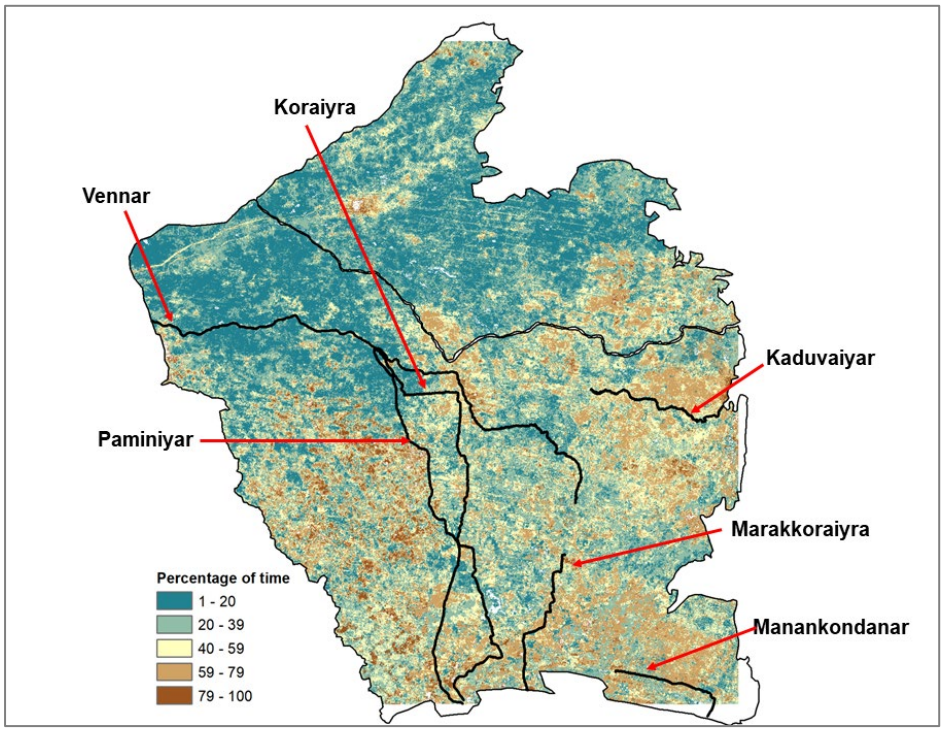

Figure 21: Relative water deficit displayed as a proportion of the Samba 2017 season across the Cauvery and Vennar command areas; black lines indicate selected river channels

91. For the Vennar River, distinct patterns of short and long water deficits (represented through the RWD parameter) are evident (Figure *22*). The head segment of the river channel (between point A and B in Figure *22*) demonstrates deficits for less of the 2017 Samba season, in comparison to the area surrounding the rest of the channel. In contrast, there are two segments which demonstrate persistent deficits during the season; these are located between points B and C on both sides of the channel, and between points D and E, also on both sides of the channel.

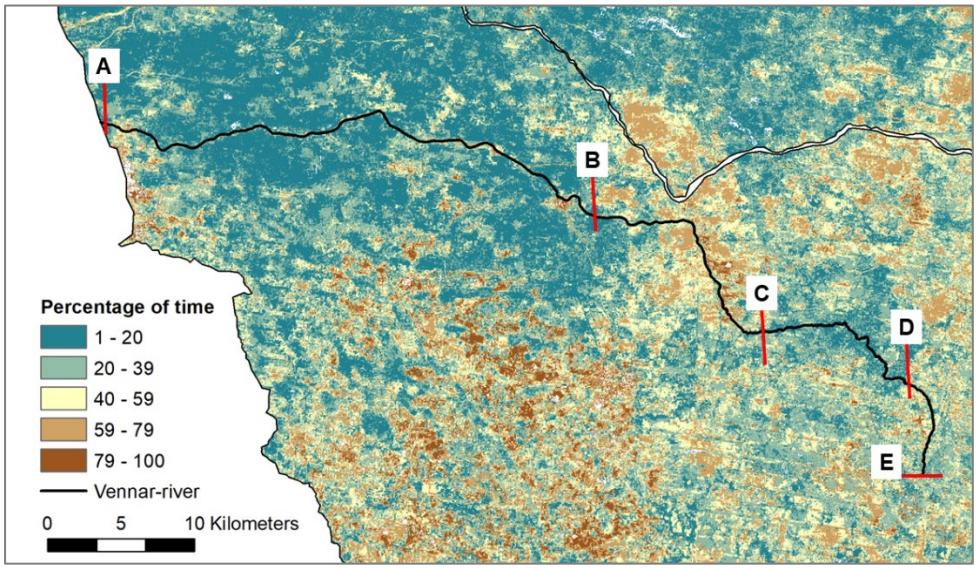

Figure 22: Distribution of water deficits (RWD=50) around the Vennar River and estimated higher and lower performing segments.

92. For the Koraiyar River, distinct patterns of water deficits of short (the blue areas) and long (the brown areas) duration are evident at the head and at the tail of the channel respectively (Figure *23*). The head segment of the river channel (between point A and B in Figure *23*) demonstrates fewer days with deficits compared to the rest of the channel. In comparison to this segment, the segment between points C and D demonstrates water deficits for a large proportion of the 2017 Samba season.

93. For the Paminiyar River, distinct patterns are also evident at the head and at the tail of the channel respectively (Figure *234*). The head segment of the river channel (between point A and B in Figure *234*) demonstrates fewer days with deficits (blue areas, <20% of the time) compared to the rest of the channel (brown areas, >40% of the time) during the 2017 Samba season. A small segment between point C and D would seem to have less issues with water supply as it demonstrates fewer deficit days (<40%) than the segments both upstream (between points B and C) and downstream (between points D and E). It is recommended to identify the possible causes for this better performance early in the detailed design phase, to better target investments here and possibly guide improvements in poorer performing segments. In addition, for this river the command areas on the western side of the river demonstrate more persistent deficits (greater number of days during the season; darker brown areas, >59%) than the areas east of the river channel.

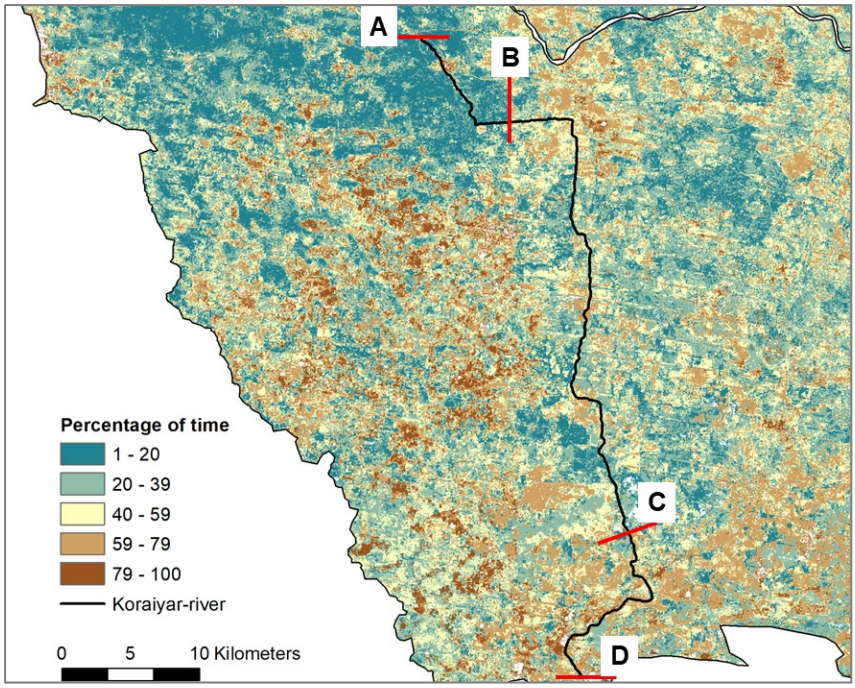

Figure 23: Distribution of water deficits (RWD=50) around the Koraiyar River and estimated higher and lower performing segments.

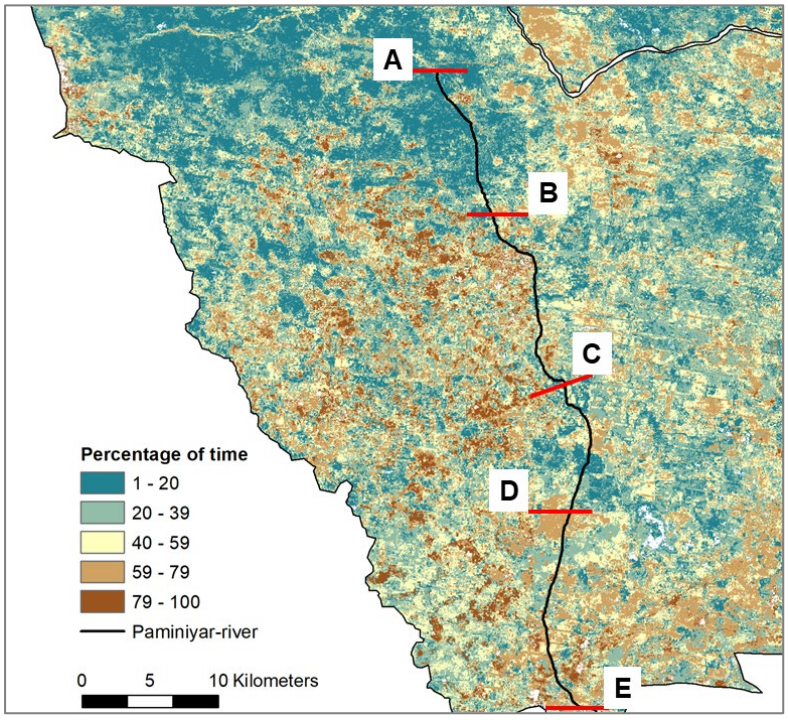

Figure 24: Distribution of water deficits (RWD=50) around the Paminiyar River and estimated higher and lower performing segments.

94. For the Kaduvaiyar River, persistent deficits during the Samba 2017 season are clear along the length of the channel (the yellow and brown areas with deficits >40% of the time, Figure *25*). Two distinct segments are visible in Figure *25*, the first is located between point A and B on the map, and the second between point B and C, with slightly higher deficits (>59%).

The second segment clearly shows greater areas of persistent deficits to the north of the river (i.e. the left bank of the channel).

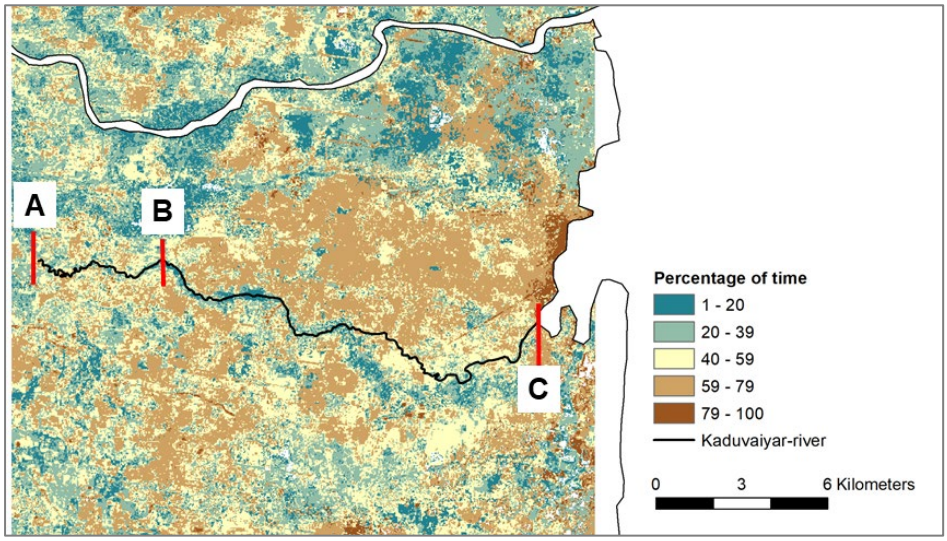

Figure 25: Distribution of water deficits (RWD=50) around the Kaduvaiyar River and estimated higher and lower performing segments.

95. The AGBP has been used as an indicator of plant growth, and as a proxy for crop production. A 10 km area on either side of the selected river channel was selected for analysis. The AGBP was classified into below average, average and above average classes of biomass and area under different classes of biomass for each buffer of the 6 targeted rivers is computed and presented in Table .

Table 10: Analysis of AGBP for selected river/canal segments.

No.	River	River Length (km)	Structures	Area within 10km buffer (km^2)	Area (%)		
					Below Avg	Avg	Above Avg
1	Paminiyar	50	81	1364	14.6	63.8	21.6
2	Manankondanar	16	2	627	28.5	62.8	8.7
3	Koraiyar	51	113	1475	11.6	66.0	22.5
4	Marakkakoraiyar	23	38	713	10.9	63.8	25.2
5	Vennar	85	111	1723	6.1	77.3	16.6
6	Kaduvaiyar	27	39	700	16.2	74.5	9.2
	Total	252	384	6603	14.7	68.0	17.3

Note: Below average (< mean – 1 standard deviation); Average - between below and above average; Above average (> mean + 1 standard deviation.

96. Analysis of the results displayed in Table indicates that each of the selected river segments showed high variability in AGBP values. On average, 68% of the areas around the selected rivers showed average biomass estimates (with in mean±sd), 15% show below average values, and 17% show above average values. The area irrigated from the Vennar

river segment showed the smallest area with below average values (6%) indicating higher production, whereas the areas around Manankondanar showed the largest areas with below average values (29%) indicating lower production. Four river segments (Paminiyar, Koraiyar, Marakkakoraiyar and Vennar) had above average biomass estimates in at least 17% of the area indicating proportionately better levels of production. On the other hand, Manankondanar and Kaduvaiyar showed greater areas with below average values (>16% of the area around these rivers) indicating lower production as compared to the other rivers analysed.

V. KEY FINDINGS

97. While a DSS is proposed to be developed for improved decision making by providing real-time information on water levels and flows in the main channels, and thus ultimately to improve irrigation water distribution to achieve equity in delivery, it is not yet at a stage where it can be used in the preparation of Project 2. Due to the current lack of in situ data to describe canal flows or irrigation water delivery, very little information is available to understand where there are problems with water delivery across the command areas, and to assist in spatial targeting of irrigation investments within the CDZ. The use of remote sensing data can be used to address this gap. We used Landsat 30 m data over 2017 Samba season to model crop water productivity parameters (such as crop evapotranspiration, above ground biomass, relative water deficit) and identify areas with lower than average productivity, and areas of persistent water deficits. The causes of this persistent water deficit should be further analysed and could inform infrastructure modernization.

98. The outputs from the analysis presented in this report have been provided to the PTAC team and are being used to assist in identifying which canals and areas should be included in Project 2, thus meeting the objective of this study to assist in prioritizing areas for investment. The analysis undertaken demonstrates the potential use of remote sensing data as a relatively low cost opportunity to fill this information gap, and to inform investments in irrigation infrastructure in areas where in situ data are unavailable or do not exist.

99. The results support the conjecture that the distribution of surface water is inefficient and inequitable with tail-end farmers not receiving adequate and reliable surface water supplies (PTAC 2018). In particular, the outputs from the analysis demonstrate a high level of temporal and spatial variability in water consumption and biomass production, and thus in water deficits and crop water productivity across the rice systems within the command area during the Samba 2017 cropping season.

100. The Vennar command area shows a higher variability and lower mean water consumption over the Samba season than the Cauvery. Within the Vennar higher values are observed in the northwest region, with a marked decline evident from northwest to southeast, towards the coast. The variations in water consumption have been characterized spatially and temporally through the use of the RWD. Within the Cauvery command area, the mean early season deficit was as high as 35% (i.e. only 65% of the demand was being met), but reducing to almost no deficit by the end of the season. Within the Vennar command area higher deficits of 20% (i.e. 80% of demand being met) still persisted towards the end of the season. There is

also a clear spatial distribution in the deficits; across the southern and eastern portion of the Vennar command, 30% of the demand was not met 70% of the time.

101. Assessment of water deficits and biomass production during the 2017 Samba season along the six selected river channels further characterizes the observed variations, and can be used to inform the selection and further assessment of high and low performing segments. The Vennar, Koraiyar, and Paminiyar all exhibit greater variability between the higher performing areas (i.e. locations where lower water deficits were identified and occurred for a lower proportion of the Samba season) at the head of the channels compared to lower performing areas (i.e. locations where higher levels of water deficit were identified and occurred for a larger proportion of the Samba season) along the length of the channels; in comparison the Manankondanar, Marakkakoraiyar and Kaduvaiyar show less variability and persistent high deficits during the season and along the entire length of the channels.

102. Analysis of distance from the irrigation channel indicates a decline in biomass production both along the length of channel as well as at a lateral distance of 10 km or higher from irrigation channels.

103. Areas of high water consumption but low biomass production are also evident across the command areas; these are characterized as areas of low water productivity, where there is an opportunity for more productive use of water or “more crop per drop”. In addition, areas of low water productivity are evident in the head sections of the channels; while irrigation water use in excess of water demand leads to low water productivity, field data and further analysis would be required to fully understand the causes and possible interventions to address this.

VI. LIST OF REFERENCES

Allen, R. G., Pereira, L. S., Howell, T. A., & Jensen, M. E., 2011. Evapotranspiration information reporting: I. Factors governing measurement accuracy. Agricultural Water Management, 98(6), 899-920.

Allen, R. G., Walter, I. A., Elliott, R. L., Howell, T. A., Itenfisu, D., Jensen, M. E., & Snyder, R. L. (Eds.). (2005, August). The ASCE standardized reference evapotranspiration equation. American Society of Civil Engineers.

Bastiaanssen, W.G.M., Menenti, M., Feddes, R.A., Holtslag, A.A.M., 1998a. A remote sensing surface energy balance algorithm for land (SEBAL). 1. Formulation. J. Hydrol. 212–213, 198–212.

Bastiaanssen, W.G.M., Pelgrum, H., Wang, J., Ma, Y., Moreno, J.F., Roerink, G.J., van der Wal, T., 1998b. A remote sensing surface energy balance algorithm for land (SEBAL).: Part 2bg d: Validation. J. Hydrol. 212–213, 213–229.

Bastiaanssen, W. G., 2000. SEBAL-based sensible and latent heat fluxes in the irrigated Gediz Basin, Turkey. *Journal of hydrology*, *229*(1-2), 87-100.

Förch W, Sijmons K, Mutie I, Kiplimo J, Cramer L, Kristjanson P, Thornton P, Radeny M, Moussa A, Bhatta G., 2013. Core Sites in the CCAFS Regions: East Africa, West Africa and South Asia, Version 3. Copenhagen, Denmark: CGIAR Research Program on Climate Change, Agriculture and Food Security

Funk, C., Peterson, P., Landsfeld, M., Pedreros, D., Verdin, J., Shukla, S., ... & Michaelsen, J. (2015). The climate hazards infrared precipitation with stations—a new environmental record for monitoring extremes. Scientific data, 2(1), 1-21.

Geethalakshmi, V., Lakshmanan, A., Rajalakshmi, D., Jagannathan, R., Sridhar, G., Ramaraj, A. P., and Anbhazhagan, R., 2011. Climate change impact assessment and adaptation strategies to sustain rice production in Cauvery basin of Tamil Nadu. *Current Science*, 342-347.

Irmak, A., Allen, R. G., Kjaersgaard, J., Huntington, J., Kamble, B., Trezza, R., & Ratcliffe, I., 2012. Operational remote sensing of ET and challenges. Evapotranspiration—Remote Sensing and Modeling, 467-492.

IWMI, 2013. Spatial Database for Climate Change Vulnerability Mapping in South Asia (https://ccafs.cgiar.org/blog/newly-developed-irrigation-map-south-asia-presented#.XvjSSedS9EZ).

Jackson, R. D., Idso, S. B., Reginato, R. J., & Pinter Jr, P. J.,1981. Canopy temperature as a crop water stress indicator. *Water resources research*, *17*(4), 1133-1138.

Jaypriya, M., & Porpavai, S. (2019). Effect of crop establishment methods and irrigation scheduling on growth and yield of direct dry seeded rice. Journal of Pharmacognosy and Phytochemistry, 8(3), 459-462.

Mohandass, S., Thiyagarajan, T. M., Palanisamy, S., & Kareem, A. A., 1993. Impact of increased temperature and CO2 on rice productivity in Cauvery Delta Zone, India-A simulation analysis. Journal of Agricultural Meteorology, 48(5), 791-794.

Mul, M., Karimi, P., Coerver, H.M., Pareeth, S., Rebelo, L.M. 202. Water Productivity and Water Accounting Methodology Manual. Project report, IHE Delft Institute for Water Education, The Netherlands and the International Water Management Institute, Sri Lanka.

Parthipan, T., Ravi, V., & Subramanian, E., 2013. Integrated weed management practices on growth and yield of direct-seeded lowland rice. Indian Journal of Weed Science, 45(1), 7-11.

PTAC, 2018: Project Technical Advisory Consultants (PTAC) – CS-2 - under Climate Adaptation in Vennar Subbasin in Cauvery Delta Project (CAVSCDP) Inception Report, November 2018.

Rajesh, V., & Thanunathan, K. (2003). Effect of seedling age, number and spacing on yield and nutrient uptake of traditional Kambanchamba rice. Madras Agricultural Journal, 90(1/3), 47-49.

SCRT 2012, Season and Crop Report for Tamil Nadu (2009-2010), Department of Economics and Statistics, Government of Tamil Nadu, 2012, Online source: http://agritech.tnau.ac.in/pdf/2012/Season%20&%20Crop%20Report%202012.pdf (last accessed: June 1st, 2020).

Sushant, S., Balasubramani, K., & Kumaraswamy, K. (2015). Spatio-temporal analysis of rainfall distribution and variability in the twentieth century, over the Cauvery Basin, South India. In Environmental Management of River Basin Ecosystems (pp. 21-41). Springer, Cham.

Steduto, P., Hsiao, T. C., Fereres, E., & Raes, D. (2012). FAO Irrigation and drainage paper 66. Crop yield response to water, Food and Agriculture Organization of the United Nations.

Thangaraj, M., & Sivasubramanian, V., 1990. Effect of low light intensity on growth and productivity of irrigated rice (Oryza sativa L.) grown in Cauvery delta region. Madras Agricultural Journal, 77(5-6), 220-224.